

Global Models for Time Series Forecasting: A Simulation Study

Hansika Hewamalage*, Christoph Bergmeir, Kasun Bandara

Hansika.Hewamalage@monash.edu, Christoph.Bergmeir@monash.edu, Herath.Bandara@monash.edu

Faculty of Information Technology, Monash University, Melbourne, Australia.

Abstract

In the current context of Big Data, the nature of many forecasting problems has changed from predicting isolated time series to predicting many time series from similar sources. The availability of large sets of time series has opened up the opportunity to develop competitive global forecasting models that simultaneously learn from many time series, which have shown recently promising results in forecasting competitions, outperforming state-of-the-art univariate forecasting techniques. Nevertheless, it still remains unclear under which circumstances global forecasting models can outperform the univariate benchmarks, especially along the dimensions of the homogeneity/heterogeneity of series, the complexity of patterns in the series, the complexity of forecasting models, and the lengths/number of series. Our study attempts to address this problem through investigating the effect from these factors, by simulating a number of datasets that have controllable time series characteristics. Specifically, we simulate time series from simple data generating processes (DGP), such as Auto Regressive (AR) and Seasonal AR, to complex DGPs, such as Chaotic Logistic Map, Self-Exciting Threshold Auto-Regressive, and Mackey-Glass Equations. The data heterogeneity is introduced by mixing time series generated from several DGPs into a single dataset. The lengths and the number of series in the dataset are varied in different scenarios. Unlike in real-world datasets, the simulated environments provide complete control over the underlying datasets. We perform experiments on these datasets using global forecasting models including Recurrent Neural Networks (RNN), Feed-Forward Neural Networks, Pooled Regression (PR) models and Light Gradient Boosting Models (LGBM), and compare their performance against standard statistical univariate forecasting techniques. Our experiments demonstrate that when trained as global forecasting models, techniques such as RNNs and LGBMs, which have complex non-linear modelling capabilities, are competitive methods in general under challenging forecasting scenarios such as series having short lengths, datasets with heterogeneous series and having minimal prior knowledge of the patterns of the series. This makes these techniques promising candidates for forecasting under uncertain situations as opposed to techniques such as PR and AR models, which assume linearity of the underlying data.

Keywords: Time Series Forecasting, Global Forecasting Models, Time Series Simulation, Data Generating Processes

1. Introduction

In many industries, such as retail, energy, ride-share, and tourism, generating accurate forecasts plays a crucial role in business decision-making scenarios. For example, for retailers such as Amazon and Walmart, sales demand forecasting is important as it provides better grounds for optimising their product inventories (Wen et al., 2017a; Bandara et al., 2019). In the energy sector, demand

*Corresponding Author Name: Hansika Hewamalage, Affiliation: Faculty of Information Technology, Monash University, Melbourne, Australia, Postal Address: Faculty of Information Technology, P.O. Box 63 Monash University, Victoria 3800, Australia, E-mail address: Hansika.Hewamalage@monash.edu

forecasts are used to determine the fuel allocation, economic dispatch, and others (Mandal et al., 2006), whereas accurate service demand forecasts across different geographies are essential for industries such as tourism and healthcare (Claveria and Torra, 2014; Bandara et al., 2020a). In ride-share services such as Uber, accurate prediction of passenger demand during extreme events can help with better resource allocation and with budget planning in advance (Zhu and Laptev, 2017).

The paradigm in time series forecasting throughout decades has been to treat every time series as an independent dataset. As a result, traditional forecasting techniques are univariate, consider each time series separately and forecast it in isolation. The Exponential Smoothing State Space Model (ETS, Hyndman et al., 2008) and Auto-Regressive Integrated Moving Average Model (ARIMA, Box et al., 1994) are the most prominent examples of such methods. However, nowadays many companies are collecting large quantities of time series from similar sources routinely, such as sales in retail of thousands of different products, measurements for predictive maintenance across many machines, smart meter data across many households, etc. Though traditional univariate techniques can still deal with forecasting under these circumstances, they leave the huge potential of learning patterns across time series untapped.

Due to this reason, there has been a paradigm shift in forecasting recently, where now a set of series, as opposed to just one series, is seen as a dataset. Then, a global forecasting model (Januschowski et al., 2020) is trained across all the series in the dataset. The global model has the same set of parameters (e.g., the weights if the global model is a neural network) for all the series in contrast to a local model which has a different set of parameters for every individual series (Januschowski et al., 2020). Nowadays, such global models for forecasting are being introduced at fast pace, e.g., in the works of Wen et al. (2017b); Salinas et al. (2019); Bandara et al. (2020b). They are quickly making their way into practice, and have won all recent prestigious forecasting competitions, such as the M4 (Makridakis et al., 2020a) and M5 competition (Makridakis et al., 2020b), and all competitions held in recent years on the Kaggle platform with a forecasting task (Bojer and Meldgaard, 2020).

The premise under which these works operate, and how they explain the almost unreasonable effectiveness of global models, is that the series have to be “related” in some way (Salinas et al., 2019; Wang et al., 2019; Rangapuram et al., 2018; Wen et al., 2017a; Bandara et al., 2020b), so that the global model can extract patterns across the series. However, none of the works attempts to define or analyse the characteristics of such “relatedness.” Furthermore, global models seem to work well even in situations where series are clearly unrelated, such as the M4 forecasting competition, whose dataset is a broad mix of un-aligned time series across many different domains. The competition was won by ES-RNN, a global recurrent neural network (Smyl, 2020).

Thus, the problem of understanding when and why global forecasting models work, is arguably the most important open problem currently in time series forecasting. The first work to offer explanations in this space is the recent work by Montero-Manso and Hyndman (2020), which demonstrates theoretically that, no matter how heterogeneous the data are, there always exists a global forecasting model for any dataset that can perform equally well or even better than a collection of local models. Thus, global forecasting models are in theory not in any way more restricted than local ones, and series don’t have to be “related” for global forecasting models to perform well. However, mere existence of such a global model does not mean it is straightforward to find or construct such a model. Instead of considering relatedness, that study focuses on model complexity. Due to exploiting more data, global models can afford to be more complex than local ones while still generalising better. Montero-Manso and Hyndman (2020) then argue that the complexity of global models can be controlled mainly by using 1) more lags as inputs, 2) using non-linear, non-parametric models, and 3) using data partitioning. Those authors then proceed to confirm and illustrate their findings empirically using real-world datasets.

Despite the insights of the work of Montero-Manso and Hyndman (2020), many questions in this space are still unanswered, around under which circumstances global forecasting models work, and how model complexity is best introduced for datasets with different amounts of data complexity, data availability, and relatedness. In order to define and fully control relatedness of the time series in a dataset, we base our work on simulated time series with known Data Generating Processes (DGP).

Then, we define relatedness in terms of the parameters of the known DGPs. This also gives us full control over the complexity of the patterns in the data and the availability of data, rather than relying on real-world datasets which may contain a mixture of many different characteristics or none at all. We perform a comprehensive experimental study under controlled conditions, to carefully analyse and quantify the interplay between complexity of the DGP, complexity of the model, amount of data available, and the “relatedness” of the series.

Our study has the following key contributions. We simulate different datasets using a number of carefully chosen DGPs which cover a variety of time series characteristics, most of them closely simulating real-world scenarios. The DGPs that we have chosen vary from simple linear AR(3), to Seasonal Auto-Regressive (SAR) DGPs, to more complex and non-linear DGPs such as Chaotic Logistic Map, Mackey-Glass Equation and Self-Exciting Threshold Auto-Regressive (SETAR) models. The simulation settings that we use in our study along with the respective DGP implementations are available publicly as a code repository¹. We have designed several experimental scenarios with each one of these DGPs. To explore the effect of data availability on the model performance, we vary the amount of data in the datasets in terms of both the number of series as well as the lengths of the individual series. For different degrees of data relatedness, we investigate both homogeneous and heterogeneous settings by changing the number of DGPs mixed within the same dataset. Thirdly, we perform experiments with a number of selected global forecasting models including Recurrent Neural Networks (RNN), Pooled Regression (PR) models, Feed-Forward Neural Networks (FFNN) and Light Gradient Boosting Machines (LGBM, [Ke et al., 2017](#)) on the simulated datasets under the different experimental scenarios. The complexity of the different global forecasting models is further changed by introducing two model setups, namely the GFM.All setup where all the series are fitted using the same global model and the GFM.GroupFeature setup, which on top of the GFM.All setup involves extra features to indicate the individual DGPs the series are generated from within a heterogeneous context. Finally, the performance of the models is compared against each other as well as against the univariate techniques of AR and SETAR models. Based on the empirical evidence, an analysis is provided around the different factors which affect the performance of different global forecasting models.

The rest of the paper is structured as follows. Section 2 first details the overall methodology employed in the study including the different experimental scenarios designed. Next, Section 3 provides a brief review of the different studies which involve time series simulation, followed by the details of the DGPs involved in this study. In Section 4, we provide the details of the different forecasting techniques that are compared against each other in the study along with their data preprocessing, model training and testing information. Section 5 presents the details of the dataset characteristics along with the evaluation metrics as well as the tests for statistical significance of the performance differences between the methods. In Section 6, we present an analysis of the results of the experiments as well as a comparison of the computational times of the employed forecasting techniques. Section 7 concludes the paper with the final remarks of the overall study, the conclusions derived and the way forward.

2. Overview of the Methodology

The methodology of our study involves first simulating a number of datasets having many different characteristics. Once the datasets are simulated as required, different forecasting techniques are tested on them. We introduce a host of experimental scenarios to quantitatively explore the interplay between the complexity of different forecasting models and characteristics of the data in this manner. In our experiments, characteristics of the data are controlled along four dimensions: 1) complexity, 2) single or multiple series, 3) heterogeneity, and 4) amount of data points, whereas forecasting models are controlled using different levels of complexity. The specific details of these controlled experimental settings are explained in this section. Figure 1 gives an overview of these experimental settings

¹Currently available at: https://drive.google.com/file/d/1Q1lh4rDEZ26_-fdKT0zi3qAMo3m9tZI_/view?usp=sharing. A github link will be provided in the final version of the manuscript.

investigated in our study.

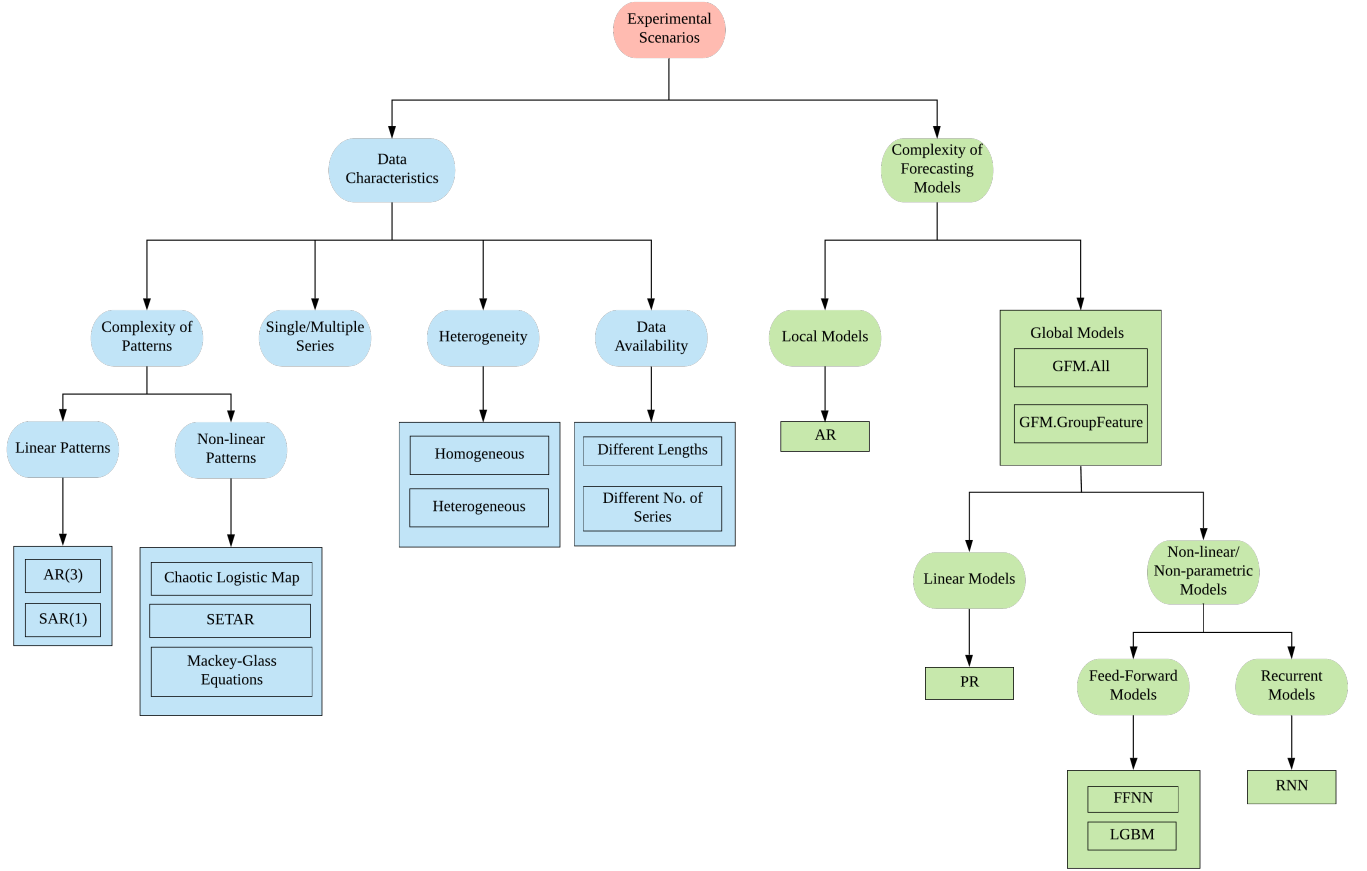


Figure 1: Visualisation of Experimental Settings Employed in the Study

2.1. Complexity of the Patterns in the Data

The complexity of the simulated time series is determined by the complexity of the underlying DGP. The different DGPs that we use for the experiments are as follows.

- AR(3)
- SAR(1)
- Chaotic Logistic Map
- SETAR
- Mackey-Glass Equation

Out of these DGPs, as discussed in more detail under Section 3, AR(3) and SAR(1) are linear DGPs whereas the rest generate time series with more complex and non-linear characteristics.

2.2. Single or Multiple Series

With every DGP used, series are both used for single series settings and split into multiple equal length series to constitute a scenario with multiple series. The purpose of this experimental scenario is to quantitatively evaluate whether it makes any difference for the models under consideration to learn from the same data either on one long series or across multiple series. For both the scenarios, we evaluate on the same forecast horizon. This means that for the multiple series scenarios, the evaluation is performed on the test forecast horizon of the series that corresponds to the last segment of the relevant long single series. In terms of the forecasting techniques, this indicates that the techniques that can be built as global models can leverage that facility when in the multiple series mode. However, for local forecasting models such as AR and SETAR models, learning is always restricted to use only one series at a time. Consequently, in single time series scenarios, such local models have more training data than in the multiple series scenarios.

2.3. Scale of Heterogeneity

We control the scale of heterogeneity of time series by simulating the following scenarios using above DGPs.

1. Homogeneous (Single) Pattern
2. Heterogeneous Patterns (Only for Multiple Series)

For multiple series, homogeneity means that all time series are simulated from the same DGP with different seeds. The multiple series scenarios can be made heterogeneous by combining time series generated from different DGPs into a single dataset. Different patterns can also be created using the same DGP by adding Gaussian noise over the coefficients. Thus, the heterogeneity experiments are performed using all DGPs, by generating each simulated time series from a new set of coefficients.

2.4. Amount of Data Available

We also control the availability of data by changing the lengths of the individual series or varying the number of series in the dataset. For single series and multiple series scenarios, this is performed using two different setups.

1. Single Series Scenarios - Varying the length of the series
2. Multiple Series Scenarios
 - (a) Homogeneous Patterns - Varying the lengths of the series, Varying the number of series
 - (b) Heterogeneous Patterns - Varying the lengths of the series

For the single series scenario, we can only change the length of the single series. However, for the multiple series scenarios with a single pattern (homogeneous), we simulate both with varying number of series and varying lengths of the series. For the multiple series scenarios with heterogeneous patterns, we only vary the amount of data by changing the lengths of the series.

Based on the different experimental considerations relevant to each DGP, such as data heterogeneity or single and multiple series inclusion, we introduce the terminology summarised in Table 1 that is used throughout the rest of this paper.

2.5. Complexity of Forecasting Techniques

The modelling capability of models is varied by conducting experiments using a number of techniques with different attributes as explained more under Section 4. The complexity of these base models can be further increased by using two techniques. The first is by increasing the number of parameters in the model. For NNs, the hyperparameters are tuned by using automated hyperparameter tuning techniques. However, the size of the input window can be increased as required to improve the complexity. For pooled regression models this can be done by increasing the lag size. The second approach is to introduce different training paradigms for GFMs as mentioned below.

Abbreviation		Meaning
SS		Single Series
MS-Hom-Short	Many Series Homogeneous with Short Lengths	
MS-Hom-Long	Many Series Homogeneous with Long Lengths	
MS-Het	Many Series Heterogeneous	

Table 1: Explanations of Abbreviations

1. GFM.All: Where the global models are trained using all the series available in the dataset irrespective of their potential heterogeneity. This setup is used in all the multiple series experimental scenarios.
2. GFM.GroupFeature: Where the global models are trained using all the series available in the dataset similar to the GFM.All setup, but in addition to the time series data, every input has an additional feature to indicate which subgroup the particular series belongs to. This approach is used to attend to existing heterogeneity in the data. It can act as an implicit clustering of the data by giving information to the models of the existence of different subgroups. However, this training paradigm is irrelevant for the heterogeneous setting that we described before, since none of the series in the dataset share coefficients. Therefore, we introduce a separate experimental scenario named Group Feature setup where we mix few patterns from each DGP within a dataset.

The GFM.All setup is the base setup. The GFM.GroupFeature setup is expected to increase the complexity of the GFM.All setup.

3. Data Generating Processes

Generating synthetic datasets is a heavily used approach in many domains to evaluate the performance of different algorithms, against other benchmarks. For example, in the domain of time series classification, [Sun et al. \(2019\)](#) generate synthetic datasets using the Lorenz system, to empirically prove the competence of their proposed algorithm that uses covariance matrices as the considered features for the classification, which makes it interpretable. On the other hand, [Zhao and Itti \(2018\)](#) simulate artificial time series by stretching and scaling original time series in order to demonstrate the capability of their newly proposed variant of DTW, which is shapeDTW for sequence alignment.

There are a number of research works which involve time series simulation for forecasting as well. [Bergmeir and Benítez \(2012\)](#) and [Bergmeir et al. \(2018\)](#) use simulated time series to investigate the validity of cross-validation for time series forecasting. [Hyndman et al. \(2002\)](#) simulate time series using ETS models and later use these series to fit ETS models and thus, evaluate the accuracy of the model selection process employed in the automated ETS models. [Petropoulos et al. \(2014\)](#) simulate time series in their study with the overall objective of identifying dominant factors in time series data that result in improved or degraded forecasting accuracies in several univariate forecasting methods and their combinations. Specifically, they simulate fast-moving data with the factors seasonality, trend, cycle, randomness, number of observations, and forecasting horizon, as well as intermittent data by considering the factors inter-demand interval, coefficient of variation, number of observations, and forecasting horizon.

Simulation studies have also been used to evaluate NNs and other Machine Learning (ML) algorithms for forecasting. [Lau and Wu \(2008\)](#) use simulations of complex, chaotic time series to demonstrate the competitive performance of their novel Support Vector Regression (SVR) model for forecasting non-linear time series. [Ye and Dai \(2021\)](#) use synthetic datasets simulated using Lorenz system to evaluate their novel transfer learning scheme for time series forecasting using Convolution Neural Networks (CNN) as the underlying deep learning architecture. Similarly, [Vanli et al. \(2019\)](#) too use simulations of delay differential equations based series, specifically Mackey-Glass and Chua’s

circuit series to assess the performance of their incremental decision tree method on sequential non-linear regression problems. In their study, [Fischer et al. \(2018\)](#) perform simulation of time series data using eight linear and non-linear DGPs such as AR models, Threshold Auto-Regressive (TAR) models and Smooth Threshold Auto-Regressive (STAR) models to evaluate the performance of the eight ML algorithms multilayer perceptron (MLP), logistic regression, naive Bayes, k-nearest neighbours, decision trees, random forests and gradient-boosted trees. To make the evaluation process more robust to outliers, from each DGP, 1000 series are generated and results averaged over the 1000 cases. Although their study develops global forecasting models, they consider forecasting as a classification problem by classifying whether the time series rises or remains constant at time t . [Zhang and Qi \(2005\)](#) use time series simulation to address specific questions related to NNs for one-step-ahead forecasting. In particular, they attempt to investigate the capability of NNs to model seasonality and trend, whether data preprocessing is required prior to feeding the data into NNs and the benefit of using NNs over the traditional forecasting method ARIMA on seasonal time series. However, they build NNs in a univariate manner where one model is built per each series. [Zhang \(2007\)](#) uses a simulation study to measure the performance of his proposed univariate ensemble FFNN with jittered training data to augment the original set of training data. The time series simulation is carried out in terms of several DGPs including AR processes, Auto-Regressive Moving Average (ARMA) processes, Non-linear AR (NAR) processes, and STAR processes. [Zhang et al. \(2001\)](#) specifically simulate non-linear time series using non-linear DGPs such as Sign AR processes, TAR models, NAR models, Non-linear Moving Average (NMA) models and STAR models to assess the effect from the input nodes, hidden nodes of NNs, and sample size on the forecasting accuracy of FFNNs in comparison with ARIMA models. Similar to this, [Suhartono et al. \(2018\)](#) also perform a study using non-linear seasonal time series simulated with an Exponential Smooth Transition Auto-Regressive (ESTAR) model to explore determining factors such as the inputs and the number of neurons in the hidden layers on the FFNN’s forecasting accuracy.

However, most of the work present in the literature builds univariate models for forecasting as opposed to global forecasting models. Most importantly, none of these studies clearly investigates how the simplicity/complexity of the series, complexity of the models, the heterogeneity/homogeneity of the data or the amount of data overall/per series affects the forecasting performance of global models. On the other hand, many of the recent studies involving global forecasting models such as RNNs, claim that global models only work with sets of related time series ([Salinas et al., 2019](#); [Wen et al., 2017b](#); [Bandara et al., 2019](#); [Januschowski et al., 2020](#)). The study by [Bandara et al. \(2020b\)](#) uses special clustering mechanisms to group the related time series together to build global models on every cluster. However, the notion of relatedness is not well-understood in many of these contexts. No proper efforts have been made to analyse these terms within controlled experimental settings. Therefore, in this study, we strive to explore the effect of these different factors for building global forecasting models in comparison to other state-of-the-art univariate forecasting benchmarks.

In the R programming language ([R Core Team, 2020](#)), there are several packages that provide the facility to simulate time series with many different statistical models. Table 2 summarises these packages along with their respective functions. The underlying statistical models that these DGPs use include ARIMA models, Seasonal ARIMA (SARIMA) models, ETS models, Complex Exponential Smoothing (CES) models, Generalized Exponential Smoothing (GES) models, Simple Moving Average (SMA) models, Vector Exponential Smoothing (VES) models, TAR models and SETAR models. Unlike the other models, the Regime Switching models SETAR and TAR allow for creating structural change in the time series, thereby creating a non-linearity in the resulting time series. The number of thresholds determines the number of regimes in the series where every individual regime is modelled by a different AR process. However, not all these statistical models are easy to use in simulating series. For complex models such as CES, GES and others, [Svetunkov \(2019\)](#) recommend to always first fit the model of choice to a real time series and then use the derived coefficients to simulate new series. This is mainly because such complex models have many different parameters which are hard to control, and therewith it is hard to estimate a reasonable value for those parameters to obtain realistic time series.

Our interest in this study lies specifically around those methods that can generate time series with controllable features, rather than random generation processes. The experimental settings of our study

R Package	Function	Details
<code>forecast</code> (Hyndman and Khandakar, 2008)	<code>simulate</code>	Generates series given fitted models from <code>ets</code> , <code>auto.arima</code> , and others.
<code>stats</code> (R Core Team, 2020)	<code>arima.sim</code>	Generates series given the AR, MA coefficients for an ARIMA model.
<code>CombMSC</code> (Smith, 2019)	<code>sarima.Sim</code>	Generates series given the AR, MA coefficients for a SARIMA model.
<code>smooth</code> (Svetunkov, 2019)	<code>sim.es</code>	Generate series out of ETS, CES, SARIMA, GES, SMA and VES models.
	<code>sim.ces</code>	
	<code>sim.ssarima</code>	
	<code>sim.gum</code>	
	<code>sim.sma</code>	
<code>tsDyn</code> (Fabio Di Narzo et al., 2019)	<code>sim.ves</code>	Generates series from a SETAR model. Either bootstraps given a series or simulates given the coefficients.
	<code>setar.sim</code>	
TAR (Zhang and Nieto, 2017)	<code>simu.tar.norm</code>	Generates series either from a TAR model or log-normal TAR model with Gaussian distributed errors, given the orders and coefficients of AR processes, the number of regimes and the thresholds.
	<code>simu.tar.lognorm</code>	
<code>gratis</code> (Kang et al., 2020b)	<code>generate.ts</code>	Generates series from MAR models given the frequency and the number of mixing components. Either generates diverse series or series having a set of tsfeatures pre-specified.
	<code>generate.ts.with.target</code>	

Table 2: Data Generation Processes in the R Programming Language

involve scenarios with simple/complex patterns, homogeneous/heterogeneous series, varying number of series, and varying series lengths, as described under Section 2. The DGPs that we use for the study are selected such that they can simulate practical forecasting scenarios as closely as possible. We start from the simplest forms of DGPs, which are linear DGPs with short memory. Then, we gradually make them more complex by increasing the number of lags to have linear DGPs with longer memory. Next, we introduce more complex, non-linear DGPs namely, a threshold linear model that switches between different linear models based on certain conditions, a chaotic model and another delay differential equation based model, the Mackey-Glass Equations. This section gives details of these DGPs that we use for our experiments in order to control the complexity of the patterns in the data.

3.1. Linear Auto-Regressive Models

We first simulate series using AR models. ARIMA models attempt to model the autocorrelation in the data (Hyndman and Athanasopoulos, 2018). AR models use a linear combination of the past values of the target series itself as regressors to predict the future values. MA models, on the other hand, model the future in terms of a linear combination of the past forecast errors. AR and MA models, once combined together with sufficient differencing of the time series to achieve stationarity, are called ARIMA models. The number of lags used for the AR model (p) and the MA model (q) and the amount of differencing (d) defines the complexity of the underlying ARIMA model. ARMA models can be approximated by pure AR models using many lags (Kang et al., 2020a). In this study, we generate series from AR models to enforce linear relationships in the simulated data. For the convenience of explanation, we first introduce the backshift operator as in Equation 1.

$$\begin{aligned}
By_t &= y_{t-1} \\
B(By_t) &= B^2y_t = y_{t-2}
\end{aligned} \tag{1}$$

The backshift operator on the variable y_t is used to denote its lags.

3.1.1. Non-Seasonal Auto-Regressive Models

Equation 2 defines a non-seasonal AR model of order p using the backshift operator.

$$y_t = c + \phi_1 B y_t + \phi_2 B^2 y_t + \phi_3 B^3 y_t + \dots + \phi_p B^p y_t + \epsilon_t \quad (2)$$

Here, ϵ_t indicates a white noise error term, which is the error in the AR modelling, and c is a constant term which is also known as the intercept. As Equation 2 shows, an AR model is a simple linear regression model where the past lags are the predictors of the value of the series at the t^{th} time step. Therefore, AR DGPs can simulate those time series common in the real world where the value at a certain time is a (linear) function of its own past values. Given a particular time series, the coefficients $\phi_1, \phi_2, \dots, \phi_p$ are estimated to fit an AR model by minimising a loss criterion such as the Maximum Likelihood Estimation (MLE). Similarly, given the values for the coefficients $\phi_1, \phi_2, \dots, \phi_p$ of the different lags, the AR model can simulate series.

In this study, we use an AR(3) DGP to simulate simple linear patterns in the time series data. For this, we use the `arima.sim` function from the `stats` package of the R core libraries (R Core Team, 2020). Since the DGP takes some time to reach stability in its generated values, to avoid issues from initial values of the DGP, a burn-in period of 100 points is cut off from the beginning of the series. The `arima.sim` function is provided with AR coefficients generated for a stationary process. Rather than generating coefficients randomly and checking for their stationarity, we follow the procedure of Bergmeir and Benítez (2012) to randomly produce the roots of the characteristic polynomial first and then generate the AR coefficients based on those. To obtain a stationary AR process, the coefficients should be such that the absolute values of the characteristic polynomial roots are greater than one (Cryer and Chan, 2008). Therefore, we first sample the roots of the characteristic polynomial randomly from a uniform distribution in the range $[-root_{max}, -1.1] \wedge [1.1, root_{max}]$ where $root_{max}$ is set to 5 (Bergmeir and Benítez, 2012). Once the series are generated in this manner, some further processing is done on them according to the work of Bergmeir et al. (2014). First, the series are normalised to zero mean and unit variance. Then, to make the scenarios more realistic we make all the data non-negative by subtracting from every series its smallest value if that is negative. Since according to Hyndman and Koehler (2006) the error measures associated with the study such as Symmetric Mean Absolute Percentage Error (SMAPE) are prone to issues with values close to zero, as the next step we add one to the whole series if the minimum value is less than one. The series from the simple AR(3) DGPs are generated likewise.

3.1.2. Seasonal Auto-Regressive Models

To make the patterns more complex, we also simulate series using an SAR model. Equation 3 shows such an SAR model of order P , where the period is denoted by S .

$$y_t = c + \Phi_1 B^S y_t + \Phi_2 B^{2S} y_t + \Phi_3 B^{3S} y_t + \dots + \Phi_P B^{PS} y_t + \epsilon_t \quad (3)$$

Comparing Equation 2 with Equation 3, in the Seasonal AR model, the predictor variables are now seasonal lags as opposed to normal lags as in the non-seasonal AR model. Therefore, the Seasonal AR model is a regression model where the predictor variables are seasonal lags of the time series. Thus, an SAR DGP can simulate time series having a seasonality of a particular periodicity which are also very commonly seen in real-world scenarios. Similar to the non-seasonal AR model, given the values of the coefficients $\Phi_1, \Phi_2, \dots, \Phi_P$, the model can simulate new time series. However, unlike in simple AR models, since it is the seasonal lags that are significant in the SAR models, they account for much longer-term dependencies, thus generating series with longer memory.

In our study, to generate series with SAR models, we first fit an SAR model of order 1 to the `USAccDeaths` monthly series of the `datasets` package (R Core Team, 2020) available in the R core libraries. The `USAccDeaths` series contains the monthly totals of accidental deaths in the USA for the period from the year 1973 to 1978, with 72 data points (Brockwell and Davis, 1991). This series shows strong yearly seasonal patterns as shown in Figure 2.

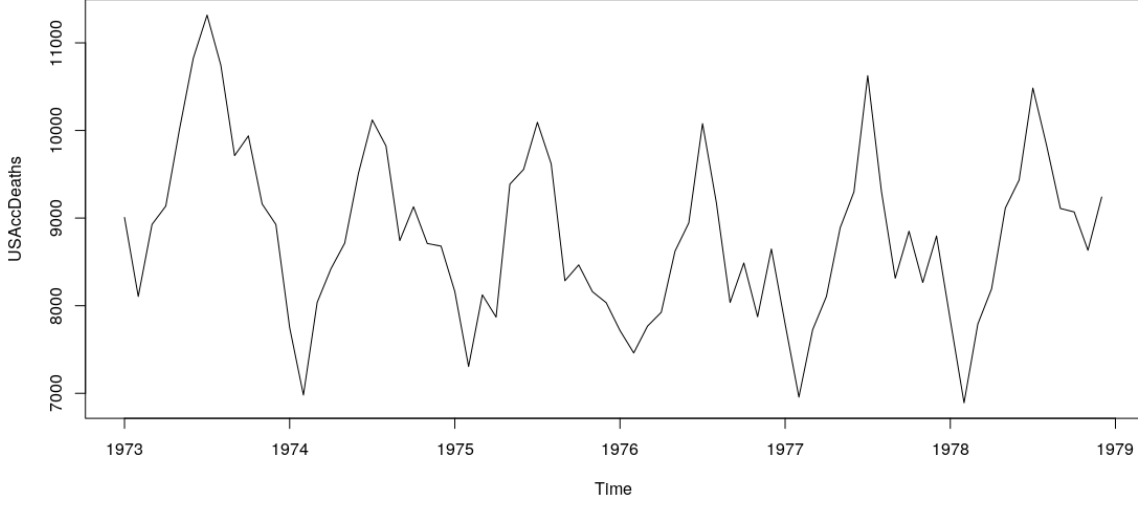


Figure 2: USAccDeaths Monthly Series with Yearly Seasonality

We use this real-world series in this case as the base series for the homogeneous experimental settings, since that ensures the expected seasonality with long memory in the generated series, rather than randomly picking coefficients. The formula of the SAR(1) model fitted to the `USAccDeaths` series is as shown in Equation 4. The value of the coefficient Φ_1 for this model is 0.85, which is close to 1 and thus resulting in significant long term memory in the series. The series in this case are simulated using the `simulate` function of the `forecast` package (Hyndman et al., 2020) by using the model fitted to the `USAccDeaths` series as the underlying DGP. A burn-in period of 100 is used to reduce the effects from initial values.

$$y_t = 9072.24 + 0.85By_t \quad (4)$$

Similar to the AR(3) DGP scenario, here also we scale the generated series to zero mean, unit variance and make all the data points greater than one. For the scenarios which introduce heterogeneity into the datasets, we also use the `sim.ssarima` function of the `smooth` package (Svetunkov, 2019) to simulate series with different SAR coefficients for every new series. The coefficients in the latter case are randomly sampled from the Uniform Distribution $U(-0.5, 0.5)$.

3.2. Chaotic Logistic Map

The Chaotic Logistic Map DGP is another technique used in this study to generate more complex patterns in the time series data. This type of logistic models were first introduced in biological research to describe the population growth of certain species over time (May, 1976). Chaos theory is used in mathematics to deal with heavily non-linear dynamical systems. Thus, Chaotic Logistic Maps are well-suited techniques for simulating non-linear characteristics in time series which can also be found in the real world. The DGP used in this study generates data as per Equation 5.

$$y_t = \max \left(ry_{t-1} (1 - y_{t-1}) + \frac{\epsilon_t}{10}, 0 \right) \quad (5)$$

This is a zero-bounded chaotic process where ϵ_t indicates a white noise error term. In this study, the datasets generated from the Chaotic Logistic Map DGPs may have zero values. We have specifically chosen the coefficient $r = 3.6$ and the initial value $y_0 = 0.5$ in all homogeneous series scenarios. This

is because, for logistic maps the chaotic behaviour is heavily observed for $r \approx 3.6$. In this way, for all homogeneous cases, we make the simulated time series difficult to model by forecasting techniques. However, for heterogeneous datasets where different coefficients are involved, r and y_0 are chosen randomly from the Uniform Distributions $U(0, 4)$ and $U(0, 1)$, respectively, to align with findings from the literature (May, 1976). Similar to other DGPs, a burn-in period of 40 points is introduced to reduce the effects of initial values.

3.3. Self-Exciting Threshold AutoRegressive Models

The SETAR model is also a technique used for simulating complex patterns. This model belongs to the family of TAR models, first introduced by Tong (1978). A TAR model is defined as in Equation 6.

$$y_t = \begin{cases} c_1 + \phi_1^1 B y_t + \phi_2^1 B^2 y_t + \phi_3^1 B^3 y_t + \dots + \phi_p^1 B^p y_t + \epsilon_t, & \text{if } z_t \leq r_1 \\ c_2 + \phi_1^2 B y_t + \phi_2^2 B^2 y_t + \phi_3^2 B^3 y_t + \dots + \phi_p^2 B^p y_t + \epsilon_t, & \text{if } r_1 \leq z_t \leq r_2 \\ \vdots & \\ \vdots & \\ c_k + \phi_1^k B y_t + \phi_2^k B^2 y_t + \phi_3^k B^3 y_t + \dots + \phi_p^k B^p y_t + \epsilon_t, & \text{if } r_{k-1} \leq z_t \end{cases} \quad (6)$$

According to Equation 6, the TAR model involves $k - 1$ number of threshold values $(r_1, r_2, \dots, r_{k-1})$, which separate the space into k regimes, where each one is modelled by a different AR process of order p . The threshold variable is denoted by z_t which is an exogenous variable. Therefore, in contrast to linear AR models, TAR models capture non-linear dynamics in time series by means of a regime-switching technique that changes the underlying AR coefficients, when a particular threshold value is met. When the threshold variable z_t is a lagged value of the series itself (denoted by y_{t-d} , where d is the delay parameter), the model is known as a SETAR model. The SETAR models were first introduced by Tong and Lim (1980). Due to their regime-switching nature, SETAR models can capture, for example, real-world scenarios where patterns of a certain time series change due to policy interventions upon reaching a certain threshold value in the time series.

For this study, we use the simulation capability of SETAR models implemented in the `setar.sim` function of the `tsDyn` R package (Fabio Di Narzo et al., 2019). To avoid the practical difficulty of ensuring that the simulated series reaches the chosen threshold at a certain point, we use the AR coefficients and the threshold values presented in the example of the `tsDyn` package. This includes two AR(2) processes with coefficients $(c_1 = 2.9, \phi_1^1 = -0.4, \phi_2^1 = -0.1)$ and $(c_2 = -1.5, \phi_1^2 = 0.2, \phi_2^2 = 0.3)$ along with a single threshold value of 2 and initial values (2.8, 2.2). This is the case for all homogeneous experimental scenarios. On the other hand, for the heterogeneous scenarios, if we randomly generate AR coefficients, threshold values and initial values, we again face the issue of ascertaining whether the simulated observations go beyond the respective threshold value. Therefore, instead of generating coefficients randomly in this manner, to create the heterogeneous datasets of this DGP, for every new series we add a small amount of random noise to the initial coefficients. While doing so, it is also essential to retain the coefficients within the stationary bounds of the AR processes. Therefore, to meet all these requirements, the amount of noise added to the coefficients is sampled from a Normal Distribution of the form $N(0, 0.007)$. Similar to the AR(3) DGP, once the series are generated, they are z-score normalised and made greater than one.

3.4. Mackey-Glass Equation

The Mackey-Glass Equation forms another DGP that can be used to simulate complex patterns in time series data. This equation was first introduced in a research studying first-order non-linear Differential-Delay Equations (DDE) which describe physiological control systems (Mackey and Glass, 1977). The Mackey-Glass Equation was specifically used to explain the fluctuations of white blood cells in the human body under certain cases of chronic leukemia. The solutions of these DDEs can be

Simulation Technique	Function	Package	Linearity
AR(3)	<code>arima.sim</code>	<code>stats</code> (R Core Team, 2020)	✓
SAR(1)	<code>simulate</code>	<code>forecast</code> (Hyndman et al., 2020)	✓
	<code>sim.ssarima</code>	<code>smooth</code> (Svetunkov, 2019)	
Chaotic Logistic Map	-	-	✗
SETAR	<code>setar.sim</code>	<code>tsDyn</code> (Fabio Di Narzo et al., 2019)	✗
Mackey-Glass Equation	<code>data.mackey_glass</code>	<code>nolitsa</code> (Mannattil, 2017)	✗

Table 3: Summary of Techniques Used for Time Series Simulation

chaotic and thus cause complexity in the underlying time series. The Mackey-Glass equation is defined as in Equation 7.

$$\frac{dy_t}{dt} = \frac{\beta y_{t-\tau}}{1 + y_{t-\tau}^n} - \gamma y_t \quad (7)$$

In Equation 7, τ is called the delay whereas $\beta, \gamma, n > 0$ are parameters that determine the periodicity and the chaos induced into the resulting series. Following from Equation 7, the solution to the Mackey-Glass equation is as shown in Equation 8.

$$y_{t+1} = y_t + \frac{\beta y_{t-\tau}}{1 + y_{t-\tau}^n} - \gamma y_t \quad (8)$$

Therefore, Equation 8 can be directly used to simulate complex time series. For this study we use the Mackey-Glass based time series generation implemented in the `nolitsa` Python package (Mannattil, 2017). Most of the publicly available implementations of Mackey-Glass based series generation use $\beta = 0.2, \gamma = 0.1, n = 10$, and $\tau \geq 17$. These are also the default values in the `nolitsa` package, with τ being equal to 23. Usually, $n \approx 10$ are the values which create chaos in the resulting series. Following common practice, we use the default values of the parameters in the `nolitsa` package to generate series for all homogeneous scenarios. As for the heterogeneous cases, the values for β, γ , and n are retained at the defaults to ensure chaos while τ is sampled randomly from the Uniform Distribution $U(17, 100)$. Once generated likewise, the series are shifted to eliminate small values below 1.

Table 3 provides an overall summary of the aforementioned techniques used for time series simulation. Here, the *Function* and *Package* columns provide the references to the respective software implementations of the simulation techniques used in our experiments. The Chaotic Logistic Map DGP is implemented by ourselves and does not involve any already existing software packages. The table furthermore indicates a characterisation of the generated time series in terms of their linearity.

4. Forecasting Framework

Depending on the specific experimental scenario, we train models either as univariate models or global forecasting models. In this section, the details of the different forecasting techniques employed are explained along with their associated data preprocessing methodologies, model training and testing.

4.1. Forecasting Techniques

For the forecasting techniques of the study, we use RNNs, FFNNs, PR models, LGBMs, AR, SETAR and SAR models as appropriate. The details of these techniques are as follows.

4.1.1. Recurrent Neural Networks

RNNs are a type of NNs that are specialised for sequence modelling problems due to their states which are propagated up to the end of the sequence and thus help them distinguish between every individual series among a set of series. Like other NNs, RNNs too are universal approximators meaning that they are inherently non-linear models (Schäfer and Zimmermann, 2006). RNNs can be implemented with many different architectures. In the study by Hewamalage et al. (2020), those authors have identified the Stacked architecture as the generally best RNN architecture across a number of real-world datasets. Therefore, in this study we choose that same architecture along with residual connections. Residual connections were introduced by He et al. (2016) on CNNs mainly for the purpose of image recognition. Such networks were named as Residual Nets (ResNets). However, later many other domains were inspired by this architecture and implemented different modified versions of it for their own work. For the time series forecasting domain, Smyl and Kuber (2016a) used residual connections on RNN layers. Moreover, the winning solution by Smyl (2020) at the M4 forecasting competition also involved RNNs with residual connections. Inspired by this work, we use an architecture similar to the work of Smyl and Kuber (2016a) in our study. In particular, our RNN architecture is illustrated in Figure 3.

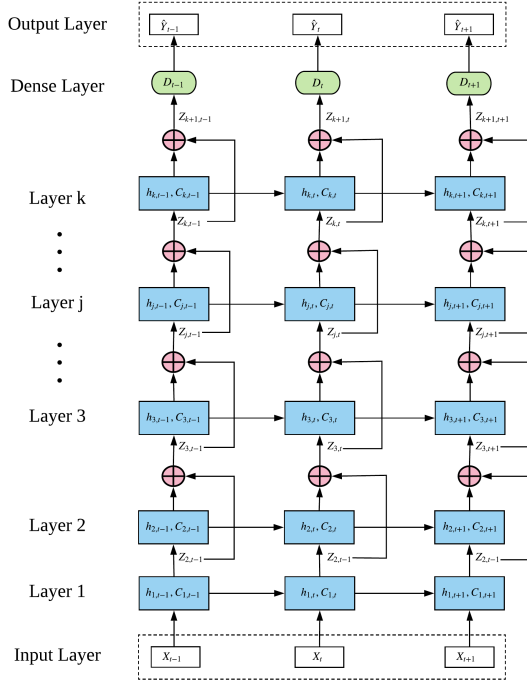


Figure 3: Recurrent Neural Network with Residual Connections

The recurrent unit used for the RNN layers in this study is the Long Short-Term Memory (LSTM) cell with peephole connections introduced by Gers et al. (2003). As shown in Figure 3, residual connections operate as a form of shortcut connections between layers. Specifically in this scenario, it allows to connect the input of one layer to the input of the next immediate layer in the stack, in addition to the usual information flow along the layers. The residual block which sits in-between layers, performs a simple addition of the output of one layer with the input of that same layer. Equation 9 demonstrates this concept where $Z_{j,t} \in \mathbb{R}^d$ represents the input to the layer j and $h_{j,t} \in \mathbb{R}^d$ represents the output from the layer j at the time step t , d being the cell dimension. For LSTM cells, $h_{j,t}$ is also the hidden state of the layer j whereas $C_{j,t}$ indicates the cell state at the time step t . Thus, the

residual connections start from the second layer, since the input to the first layer $X_t \in \mathbb{R}^m$ is of the input window size and the rest has the size of the cell dimension which makes it impossible to perform an addition operation between them.

$$Z_{j,t} = h_{j-1,t} + Z_{j-1,t} \quad (9)$$

The residual connections are especially helpful to avoid vanishing gradient issues of the layers of NNs. This is because, with residual connections, the output of every layer $h_{j-1,t}$ corresponds to a residual mapping in addition to the identity mapping performed by the connection from the input $Z_{j-1,t}$. Therefore, even if the upper layers perform very poorly, the final output would be at least as good as the initial input. In other words, the final error of the overall network should not go beyond the error from its shallow counterparts. In contrast, in the usual Stacked architecture as in the work of Hewamalage et al. (2020), the stack of layers attempts to model the final expected mapping. He et al. (2016) also state that it is easier for layers to learn a residual mapping than the true underlying mapping. The benefit of these shortcut connections is that they come with no cost of additional trainable parameters. On top of the final layer of the RNN with k layers, an affine neural layer (fully connected layer without a bias vector) indicated by D_t exists which converts the output from the RNN $Z_{k+1,t} \in \mathbb{R}^d$ into the final output \hat{Y}_t having the size of the expected forecasting horizon H . The RNNs used for this study are implemented with version 2.0 of the Tensorflow open-source deep learning framework (Abadi et al., 2015).

4.1.2. Feed-Forward Neural Networks

An FFNN can be described as the most basic type of an NN. The neurons within a single layer of an FFNN have no feedback connections as in an RNN and the neurons of each layer feed their outputs directly into the next immediate layer of the stack. Thus, FFNNs, when used for forecasting problems as described here, do not differentiate between individual time series as an RNN, since they do not have per-series states that propagate towards the end of the series. FFNNs can only distinguish between windows in a moving window scheme later explained in detail under Section 4.2.3.

The layers that we use in the FFNNs are fully connected. Figure 4 depicts the general architecture of the FFNNs used in this study. In Figure 4, m and n denote the input and output window sizes, respectively, where l indicates the total number of layers including the output layer. As shown in Figure 4, the number of nodes in the input and output layers correspond to the input and output sizes of the windows.

$$z_i^j = w_i^j \odot A^{j-1} + b_i^j \quad (10a)$$

$$a_i^j = f(z_i^j) \quad (10b)$$

$$Z^j = W^j \odot A^{j-1} + B^j \quad (11a)$$

$$A^j = f(Z^j) \quad (11b)$$

Equation 10 defines the functionality of the i^{th} neuron of layer j in an FFNN where $z_i^j, b_i^j, a_i^j \in \mathbb{R}$ and $w_i^j, A^{j-1} \in \mathbb{R}^{k_{j-1}}$. Here, k_{j-1} denotes the number of hidden nodes in layer $j-1$ of the FFNN. w_i^j and b_i^j are the weights vector and the bias of the neuron, respectively. A^{j-1} are the final outputs at the $j-1$ layer, z_i^j is the output from the linear mapping and a_i^j is the final output from the neuron. Therefore, Equation 10a is simply a linear function of the outputs of the previous layer whereas the activation function f in Equation 10b introduces the non-linearity into the model. Although there are many options for this activation function, in our study we use the *tanh* function. Equation 11 depicts the same functionality as in Equation 10, but on the whole layer instead of just one neuron. In

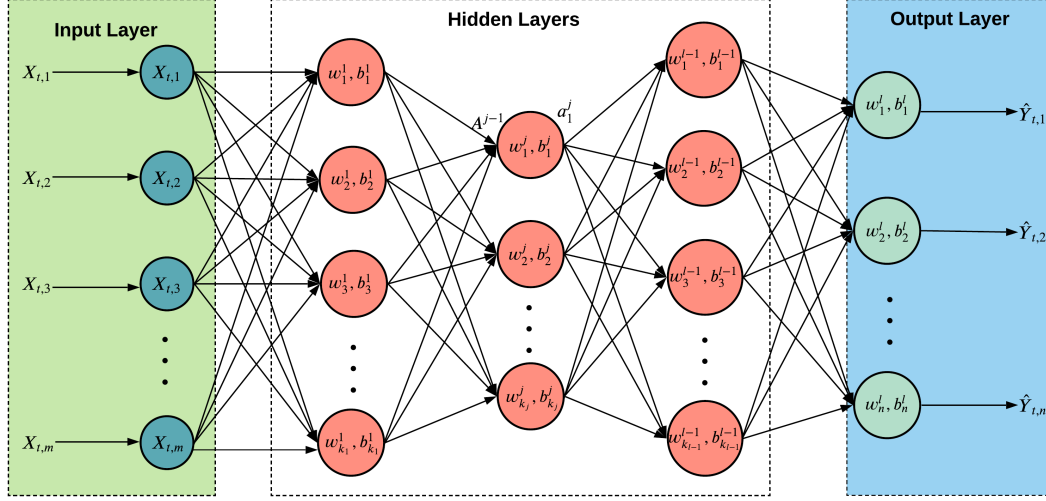


Figure 4: Feed-Forward Neural Network

Equation 11, $Z^j, B^j, A^j \in \mathbb{R}^{k_j}$, and k_j indicates the number of hidden nodes in layer j of the FFNN. $W^j \in \mathbb{R}^{k_j \times k_{j-1}}$ is the weight matrix of layer j of the FFNN and $A^{j-1} \in \mathbb{R}^{k_{j-1}}$ is as in Equation 10.

The FFNNs used for this study are implemented with version 2.0 of the Tensorflow open-source deep learning framework (Abadi et al., 2015).

4.1.3. Light Gradient Boosting Models

We also use LGBMs in our study as another forecasting technique. Extreme Gradient Boosting (XGBoost) models (Chen and Guestrin, 2016) recently have become popular by winning many ML related challenges. Gradient Boosting Models (GBM) are a type of ML algorithms based on decision trees and can be used to solve a wide range of ML problems including regression, classification, and others. As the name implies, this technique uses boosting as an ensembling approach among different decision trees. Although a quite competitive model, XGBoost can become extremely slow when fed with lots of data. This is where LGBM comes into play. As the very name suggests, LGBM is a lighter version of GBM which trains faster with fewer memory usage while achieving higher accuracy over the original GBMs (Ke et al., 2017). The key to this performance gain are two new techniques introduced in LGBM, named as the Gradient-based One-Side Sampling and Exclusive Feature Bundling which support dealing with large amounts of data with many features. The idea behind these techniques is to systematically reduce the number of data instances and features considered for computing the information gain at each split-point of the decision tree. Due to the non-linear nature of decision trees, which is the fundamental building block of LGBMs, they too are non-linear models.

The competitive performance of LGBMs when used for forecasting has been most recently demonstrated at the M5 Forecasting Competition, where an LGBM-based solution won the first place followed by many other LGBM-based solutions securing top ranks (Makridakis et al., 2020b). However, similar to FFNNs, LGBMs by default have no notion of the individual series of a dataset, when used for forecasting. They are only aware of the windows and they do not remember anything beyond what they see immediately within this input window. In our study we use the LGBM implementation available in the Python package `lightgbm` (Ke et al., 2017).

4.1.4. Linear Auto-Regressive Models

We also use univariate AR models, both non-seasonal and seasonal as other forecasting techniques in the study. The modelling process of these AR models is the same as described by Equations 2

and 3 in the format of DGPs. AR models are linear in the lags of the target series. To implement the AR and SAR models for forecasting, we use the `Arima` function of the `forecast` package in the R programming language by providing the required seasonal or non-seasonal orders (Hyndman et al., 2020).

4.1.5. Self-Exciting Threshold Auto-Regressive Models

For the scenarios involving the datasets generated from the SETAR DGP, we also experiment with SETAR as a forecasting technique. The underlying modelling process of the SETAR forecast model is as described in Equation 6 under Section 3.3 for the DGPs. Due to the inherent regime-switching nature, SETAR is a non-linear forecast model. In this study, to implement the SETAR models we use the `setar` function from the `tsDyn` package in the R programming language (Fabio Di Narzo et al., 2019).

4.1.6. Pooled Regression Models

We implement PR models similar to the work of Trapero et al. (2015) as another forecasting technique for the study. The PR model is effectively a global version of an AR model. The term pooling indicates that the coefficients of such regression models are calculated by pooling across many series. However, compared with, e.g., RNNs, the pooled regression models can only capture linear relationships in the data. Also, similar to FFNNs, PR models also do not maintain a state per every time series in the dataset. A PR model of order p can be defined as in Equation 12. This equation is the same as in Equation 2 for the non-seasonal AR model, except now the coefficients Θ are calculated by pooling across all the series in the dataset.

$$y_t = c + \Theta_1 B y_t + \Theta_2 B^2 y_t + \Theta_3 B^3 y_t + \dots + \Theta_p B^p y_t + \epsilon_t \quad (12)$$

PR models in this context are used to distinguish potential gains of using RNNs as opposed to linear models as global models. The PR models may also assist in identifying accuracy gains from purely using cross-series information without any complex architectural additions from RNNs (Hewamalage et al., 2020). To implement the PR models, we use the `glm` function in the `stats` package of the R core libraries (R Core Team, 2020).

4.2. Data Preprocessing for Forecasting

This section contains the details of all the preprocessing methods applied to the data corresponding to the different forecasting techniques.

4.2.1. Time Series Normalisation

The different time series that constitute a dataset may be in different scales. Although not quite problematic for univariate models built per each series, having series with such different scales can have adverse effects on global models (Sen et al., 2019). Therefore, we strive to normalise the series for scale before feeding into the global forecasting models by performing a mean scale transformation as done in the work of Bandara et al. (2019). This step is performed as depicted in Equation 13 where l denotes the length of the i^{th} time series, n the number of time series available and $\tilde{y}_{i,t}$, the mean scaled value of the t^{th} time step of the i^{th} time series.

$$\tilde{y}_{i,t} = \frac{y_{i,t}}{\frac{1}{l} \sum_{t=1}^{t=l} y_{i,t}} \quad \text{for } i = 1, 2, \dots, n \quad (13)$$

4.2.2. Logarithmic Transformation

In this study, we train the forecasting techniques to model the seasonality and trend components of the time series by itself, rather than extracting them from the series beforehand. This is mainly because it is our objective to perform minimal preprocessing on the data and get the models themselves to fit the data and do the forecasting as appropriate. Although not very common with the DGPs used in this study, time series may often contain exponential trends and multiplicative seasonal patterns. Especially, NNs have saturation effects after certain thresholds due to their activation functions such as \tanh . Therefore, the predicted values from NNs are anyway bounded by the limits of such transfer functions which may result in large forecasting errors especially in scenarios with exponential trends (Bandara et al., 2019). The reasons behind using logarithmic transformations are stabilising the variance in the data, scaling down the time series values and removing multiplicative seasonality components prior to applying additive seasonality decomposition techniques (Hewamalage et al., 2020). Hence, logarithmic transformations are capable of stabilising the variance in the data by removing exponential trends in time series and converting them into linear trends. Thus, in this study we use log transformation to ensure that the predictions of ML models are consistent when modelling the originally exponential trend components directly, as well as to scale down the time series further after the mean scaling step. In this study we use the log transformation analogous to the work of Hewamalage et al. (2020). This is done as indicated in Equation 14 where y_t denotes the value of the time series at the t^{th} time step.

$$w_t = \begin{cases} \log(y_t) & \text{if } \min(y) > \epsilon, \\ \log(y_t + 1) & \text{if } \min(y) \leq \epsilon \end{cases} \quad (14)$$

In Equation 14, ϵ can be defined as either zero for count data or a small positive value close to zero for real-valued data (Hewamalage et al., 2020). However, for this study, we set the value of ϵ to 0. For 0 values in the data, they are shifted by adding 1 to make the log transformation possible. This study does not involve series with negative values.

4.2.3. Moving Window Approach

The forecasting scenarios that we simulate in this study are all multi-step-ahead forecasting settings, which means that the models are required to produce forecasts for a forecasting horizon which comprises of more than one future time step. For such forecasting problems, with NNs it has been shown in the literature that the direct multi-step-ahead strategy which directly predicts the whole horizon is the best approach (Ben Taieb et al., 2012; Wen et al., 2017a; Hewamalage et al., 2020). This is mainly due to the error accumulation issues associated with the recursive schemes which use previous forecasts as the input data for the successive prediction steps. Therefore, to feed the data into the NNs (RNNs, FFNNs) in this study we employ the Multi-Input Multi-Output (MIMO) strategy enforced by the moving window scheme, as also discussed by Smyl and Kuber (2016b). For LGBMs, the same moving window input and output format is used. However, LGBMs are only capable of producing one output at a time, not multiple outputs for a window. Therefore, rather than using a recursive strategy, the training procedure for LGBMs is slightly modified as explained further in Section 4.3.3 to cater for this requirement. On the other hand, both AR models and their corresponding global version PR models use a recursive strategy by taking as input a window of time series values corresponding to the specific AR order. SETAR models too use a mechanism of recursive one-step-ahead forecasts to produce an output window. The moving window scheme implemented in this study is the same as the one from Hewamalage et al. (2020).

4.2.4. Window Normalisation

As mentioned before in Section 4.2.2, the log transformation itself supports the modelling process of machine learning models, by scaling down the values of the time series and thus reducing potential risks from saturation effects. However, when preprocessed using the moving window strategy, the time series values can be further normalised within the individual input-output window pairs. To

this end, we perform a within-window local normalisation of the data similar to the work of [Bandara et al. \(2019\)](#). Consequently, the mean of every input window is subtracted from the corresponding input-output window pair. This mechanism helps particularly in scenarios where the size of the input window is comparatively high, resulting in the last values within the input window to lie outside of the saturation regions due to trends present in the data. This local normalisation step helps NNs to produce conservative but yet responsive forecasts using their inherent saturation effects by shifting the time series values to lie within the saturation bounds ([Bandara et al., 2020b](#)). The models that use this per-window normalisation are the same as those which use the moving window scheme.

4.3. Model Training

This section presents the information specific to the training and testing procedures of ML-based forecasting techniques used in this study.

4.3.1. Recurrent Neural Networks

Throughout the study we use the stacked architecture described in Section 4.1.1 along with the COntinuous COin Betting (COCOBB) optimiser introduced by [Orabona and Tommasi \(2017\)](#) as the underlying learning algorithm for the Backpropagation Through Time (BPTT) procedure. The COCOBB optimiser relieves the user from defining an initial learning rate, which makes the whole process far more automatic. We use a Tensorflow-based implementation of the optimiser available as an open-source library ([Orabona, 2017](#)). The RNN unit that constitutes the networks is the LSTM cell with peephole connections as mentioned before in Section 4.1.1. The choice of this RNN architecture, optimiser and the recurrent cell type follows from the conclusions of a recent study by [Hewamalage et al. \(2020\)](#).

A number of hyperparameters are tuned for RNNs. However, these hyperparameters and their initial ranges are different between the scenarios which involve just a single series in the experiment and many series. For the experiments with a single series, the hyperparameters tuned include the cell dimension, the number of layers, the number of epochs, the L2 regularisation parameter, the standard deviation of the Gaussian noise added, and the standard deviation of the normal distribution from which values are randomly picked for initialisers of the network. Besides these hyperparameters, the experiments with multiple series also tune the mini-batch size and the epoch size. All these hyperparameters are used in this study in the same notion as in the work of [Hewamalage et al. \(2020\)](#). The Gaussian noise inclusion and the L2 regularisation are used as means of reducing the overfitting effects of the RNNs to the training data. The epoch size denotes the number of times that the whole dataset is repeated within one epoch. Therefore, epoch size and mini-batch size are both not relevant in the context of a single series. For tuning the hyperparameters we use the Sequential Model-based Algorithm Configuration (SMAC) tool introduced by [Hutter et al. \(2011\)](#). In particular we use the version 0.11.1 of the `smac` Python package ([Lindauer et al., 2017](#)). For the tuning of the hyperparameters of each experiment, we use 25 or 50 `smac` iterations (depending on the complexity of the experiment) while evaluating the accuracy on a validation dataset. The common initial ranges of the hyperparameters provided to the SMAC tool for both the single series and multiple series scenarios are as mentioned in Table 4.

Since the single series scenarios do not involve the epoch size hyperparameter, we need to ensure that these scenarios will still receive approximately the same amount of weight updates as the multiple series settings. Therefore, for the single series scenarios, we have increased the initial range for the number of epochs to 20-300. Since the LSTM cells themselves are complex RNN units, the number of hidden layers can be as low as 1-2, to control the complexity of the overall architecture ([Hewamalage et al., 2020](#)). The total number of series (100 for each multiple series scenario) is merely an upper limit on the mini-batch size. The actual mini-batch size is rather dependent on the available memory capacity of the system and the total computational costs. A smaller mini-batch size is expected to use a smaller memory amount at the cost of higher computation times. On the other hand, larger batch sizes take comparatively less training time at the cost of more memory. Furthermore, recent studies have demonstrated superior performance of RNNs when trained with gradient descent of mini-batch

Hyperparameter	Many Series Setting	Single Series Setting
Cell Dimension	20-50	20-50
Number of Layers	1-2	1-2
Mini-batch Size	10-100 or 1-100	-
Number of Epochs	5-30	20-300
Epoch Size	1-10	-
L2 Regularisation Param.	0.0001-0.0008	0.0001-0.0008
Std. of Gaussian Noise	0.0001-0.0008	0.0001-0.0008
Std. of Initialiser	0.0001-0.0008	0.0001-0.0008

Table 4: Initial Hyperparameter Ranges for RNNs

size 1 as opposed to other mini-batch sizes (Smyl, 2020). Depending on the scale of the different experimental scenarios employed in this study, we set the lower bound of the initial range for the mini-batch size to either 1 or 10. Due to computational constraints resulting from the long lengths of the series associated with MS-Hom-Long scenarios explained in Section 2, for those experiments we set the lower bound of the mini-batch size to 10. During every epoch of the training process, the dataset is randomly shuffled before fed into the RNN. This makes the RNN encounter the data in different sequences in every epoch and improves its generalisation capability. For the training loss in the RNNs we use the Mean Absolute Error (MAE) along with the L2 regularisation loss as per the work of Hewamalage et al. (2020).

4.3.2. Feed-Forward Neural Networks

The FFNN architecture implemented in this study is as explained in Section 4.1.2. However, unlike the RNNs, for the FFNNs, we use the well-known Adam optimiser as the underlying learning algorithm (Kingma and Ba, 2015). From a preliminary study involving few experimental scenarios, the Adam optimiser was better for the FFNNs than the COCOB optimiser. Furthermore, although the literature holds evidence for the competitive forecasting performance of RNNs with the COCOB optimiser, there is no such evidence for any FFNN architectures with respect to forecasting. Therefore, for FFNNs we use the standard built-in Tensorflow implementation of the Adam optimiser.

The initial hyperparameter ranges used for the FFNNs are as shown in Table 5. The cell dimension of RNNs is not relevant in the context of FFNNs. Apart from the other hyperparameters of the RNNs, the FFNNs also have a number of hidden nodes in each layer and the initial learning rate of the Adam optimiser which need to be tuned. The number of hidden nodes at each layer can be different from each other. To set values for the number of hidden nodes, we employ the commonly used heuristic to restrict the range in between the input window size and the output window size. In our forecasting scenarios, the output window size is always less than the input window size and the smallest output window size in any scenario is 3. Therefore, the initial range for the number of hidden nodes is varied in between 3 and the input window size in each scenario. Since the neurons in an FFNN are not as complex as LSTM cells, to increase the complexity of the overall model with respect to the RNN architectures, we set the initial range for the number of layers to be 1-5. Furthermore, for the learning rate of the Adam optimiser, a value in between 0.0001 and 0.1 is set. All the other hyperparameters are tuned analogously to the RNNs.

Apart from the architectural differences and the aforementioned hyperparameters, the training process of both RNNs and FFNNs are the same where the SMAC tool is first used to tune the hyperparameters and later, the optimal hyperparameter combination is used for model testing. The loss functions used are also similar to RNNs.

4.3.3. Light Gradient Boosting Models

As mentioned before in Section 4.2.3, LGBMs can only produce a single output. Therefore, to output windows using LGBMs, we build one model per every step in the output horizon rather than

Hyperparameter	Many Series Setting	Single Series Setting
Number of Layers	1-5	1-5
Number of Hidden Nodes	3-input size	3-input size
Mini-batch Size	10-100 or 1-100	-
Number of Epochs	5-60	20-300
Epoch Size	1-10	-
Initial Learning Rate	0.0001-0.1	0.0001-0.1
L2 Regularisation Param.	0.0001-0.0008	0.0001-0.0008
Std. of Gaussian Noise	0.0001-0.0008	0.0001-0.0008
Std. of Initialiser	0.0001-0.0008	0.0001-0.0008

Table 5: Initial Hyperparameter Ranges for FFNNs

Hyperparameter	Value
Number of Epochs	1200
Early Stopping Round	5
Learning Rate	0.075

Table 6: Hyperparameter Values for LGBMs

using a recursive strategy. This is similar to the functionality of the final layer of an NN which has a separate set of weights, and thus a separate function for every point in the forecast horizon. However, in the LGBM the whole model is different for the individual steps in the horizon. Nevertheless, the efficiency encouraged by the LGBM implementation makes this procedure computationally feasible.

Many of the hyperparameters that LGBMs have are associated with the underlying random forest, and we leave most of them at their default values as specified by the `lightgbm` Python package (Ke et al., 2017). This is mainly because, in practice the LGBM models perform quite competitively even without extensive hyperparameter tuning. To avoid the overhead of ensuring that the models do not overfit, we employ an early stopping mechanism to stop the training when an improvement in the validation error metric is not achieved over 5 consecutive epochs. The maximum number of epochs and the initial learning rate are specified as 1,200 and 0.075, respectively. These hyperparameter values are also shown in Table 6.

The LGBM implementations used in our study use the same input and output format as the NNs. However, since the LGBMs have no notion of the individual series beyond the input and output windows, the validation periods are not required to be reserved from the end of the sequences. The validity of using standard K-fold cross validation for time series forecasting in this way, is proved by Bergmeir et al. (2018) in their work. Therefore, we use a standard 7:3 split for the training and validation datasets of the LGBMs. MAE is used as the objective function for training.

4.3.4. Auto-Regressive Models

The AR models are built as local univariate models which learn only from the past values of the target series, and not across series. Unlike NNs, they are trained by considering a sequence of only one-step-ahead predictions. The loss function used for training is the default in the `forecast` package, the Maximum Likelihood Estimate (MLE), which is effectively Mean Squared Error (MSE) as a normal distribution of the errors is assumed.

4.3.5. Self-Exciting Threshold Auto-Regressive Models

Similar to the AR models, SETAR model too is built as a univariate forecasting model fitted to every individual series separately using one-step-ahead forecasts. The loss function used for the SETAR model is the default in the `tsDyn` package for the `setar` function, which is Conditional Least Squares (CLS) estimate.

Forecasting Technique	Software Details	Attributes
RNN	Tensorflow Framework (Abadi et al., 2015)	Non-linear Modelling Per Series State
FFNN	Tensorflow Framework (Abadi et al., 2015)	Non-linear Modelling
LGBM	lightgbm Python Package (Ke et al., 2017)	Non-linear Modelling
SETAR	tsDyn R Package (Fabio Di Narzo et al., 2019) (setar function)	Non-linear Modelling
PR	stats R Package (R Core Team, 2020) (glm function)	Linear Modelling
AR	forecast R Package (Hyndman et al., 2020) (Arima function)	Linear Modelling

Table 7: Summary of Forecasting Techniques

4.3.6. Pooled Regression Models

Similar to the AR models, PR models too are trained using one-step-ahead predictions. The loss function used for the PR models is Iteratively Re-weighted Least Squares (IRLS) which is the default in the `glm` function from the R package `stats` used in our experiments.

4.4. Model Testing

For the NNs, once the optimal hyperparameters are found using the hyperparameter tuning techniques as described in Section 4.3, this optimal hyperparameter combination is applied for training the NNs once again and testing on the test data. During testing, the NNs are trained using 10 Tensorflow graph seeds and then the final NN forecasts are ensembled by taking the median, as discussed by Hewamalage et al. (2020). This approach effectively addresses the parameter uncertainty associated with the NNs by initialising the networks 10 times independently.

For all the other models, once the model training is completed, the trained models are then used to perform the forecasting on the intended forecast horizon. As mentioned before, even though AR, SETAR and PR models train using one-step-ahead forecasts, during testing an output window is formed by performing a recursive strategy. LGBMs achieve the same objective by having one model per each step in the horizon.

4.5. Data Postprocessing

Once the forecasts are obtained from each individual model, a sequence of postprocessing is done on the forecasts, to reverse the preprocessing steps that were carried out on the data beforehand. This is done in the following order: 1) Add the last input point trend value back into the corresponding output windows. 2) Transform the data by taking the exponential. 3) Deduct 1, in case the original data contains zero values. 4) Re-scale the forecasts by multiplying by the series means. However, the exact postprocessing steps performed on the forecasts of each model, depend on which preprocessing was done in the beginning. The summary of all the forecasting techniques used for the study along with their respective attributes as well as the corresponding software details are available in Table 7.

5. Experimental Setup

This section details the experimental framework used in this study. To achieve significant results, for every scenario we generate 1000 datasets having the described characteristics and average the results over 1000 runs. In the rest of this section, we present the details of the datasets generation, error metrics used for the evaluation and the statistical tests conducted for the significance of the differences.

5.1. Generation of Datasets

The characteristics of different datasets generated from all DGPs according to the experimental scenarios explained in Section 2, are shown in Table 8. Here, the *Min. Length* and *Max. Length* columns refer to the range of the time series lengths we select when training our models. Similarly, *Min. No. of Series* and *Max. No. of Series* is the range of number of time series we use in our experiments. In this way, we investigate the effect of these time series characteristics on model accuracy. Due to computational constraints arising from the variety of experiments designed, out of the five DGPs used in the study, we perform the data availability experiments only using three DGPs, namely AR(3), SAR(1) and Chaotic Logistic Map. For SETAR and Mackey-Glass Equation DGPs, we experiment using only one selected length and number of series as shown in Table 8. Here, the idea is that once the important conclusions are drawn about data availability in initial experiments, those conclusions can be used to fix a sufficient length and the number of series for the remaining experiments. Also, due to the computational constraints, we perform the Group Feature setup experiments only using the Chaotic Logistic Map DGP. Our intuition here is that the analysis performed on the results of this sample experiment, is general and holds also for other DGPs. In Table 9, are the characteristics of the datasets generated for this Group Feature setup of the Chaotic Logistic Map DGP.

In the same manner that we reduce the data availability experiments as mentioned before, we also drop the number of datasets associated with each scenario to 100, to avoid heavy computational complexities of this study. This applies to the experiments on the two DGPs, Mackey-Glass Equation and SETAR and the Group Feature setup of the Chaotic Logistic Map DGP. Although the evaluation is performed on such a large number of datasets for each scenario, to make the process more efficient we tune the hyper-parameters only on one of those datasets for each scenario and apply that same optimal hyper-parameter combination in all the 100/1000 evaluations. Yet, on the one dataset where the hyper-parameters are tuned, they are tuned for all the different lengths and number of series to account for the data availability conditions.

5.2. Performance Measures

The relative performance of the models is evaluated with respect to two performance measures commonly found in the literature related to forecasting, namely SMAPE and Mean Absolute Scaled Error (MASE). Equation 15 and 16 denote the SMAPE and MASE metrics, respectively.

$$SMAPE = \frac{100\%}{H} \sum_{k=1}^H \frac{|F_k - Y_k|}{(|Y_k| + |F_k|)/2} \quad (15)$$

$$MASE = \frac{\frac{1}{H} \sum_{k=1}^H |F_k - Y_k|}{\frac{1}{T-M} \sum_{k=M+1}^T |Y_k - Y_{k-M}|} \quad (16)$$

In Equations 15 and 16, F_k and Y_k indicate the forecasts and the actual values, respectively, where H denotes the size of the forecast horizon. According to, e.g., Hyndman and Koehler (2006), the SMAPE metric is highly skewed with values close to zero. Therefore, as per the guidelines by Hewamalage et al. (2020), on the Chaotic Logistic Map DGP datasets which have zero values, we use an SMAPE variant where Equation 17 is used as the denominator of the usual SMAPE formula.

$$\max(|Y_k| + |F_k| + \epsilon, 0.5 + \epsilon) \quad (17)$$

Following the work of Hewamalage et al. (2020), we set ϵ in Equation 17 to 0.1, a small positive quantity. However, the SMAPE error metric also has other issues such as its lack of interpretability (Hyndman and Koehler, 2006). This is why we also use the MASE metric which was introduced by Hyndman and Koehler (2006).

Both SMAPE and MASE are scale-independent error measures. Furthermore, MASE is a relative error metric meaning that it measures the performance of the model with respect to the average in-sample one-step ahead error of some other standard benchmark such as the naïve forecast for data

Characteristic	SS	MS-Hom-Short	MS-Hom-Long	MS-Het
AR(3) DGP				
No. of DGPs	1	1	1	100
Min. Length	18	18	18	18
Max. Length	1800	18	180	180
Min. No. of Series	1	1	100	100
Max. No. of Series	1	100	100	100
Forecast Horizon	3	3	3	3
SAR(1) DGP				
No. of DGPs	1	1	1	100
Min. Length	24	24	24	24
Max. Length	2400	24	240	240
Min. No. of Series	1	1	100	100
Max. No. of Series	1	100	100	100
Forecast Horizon	3	3	3	3
Chaotic Logistic Map DGP				
No. of DGPs	1	1	1	100
Min. Length	60	60	60	60
Max. Length	6000	60	600	600
Min. No. of Series	1	1	100	100
Max. No. of Series	1	100	100	100
Forecast Horizon	12	12	12	12
SETAR DGP				
No. of DGPs	1	1	1	100
Min. Length	6000	60	240	240
Max. Length	6000	60	240	240
Min. No. of Series	1	100	100	100
Max. No. of Series	1	100	100	100
Forecast Horizon	12	12	12	12
Mackey-Glass Equation DGP				
No. of DGPs	1	1	1	100
Min. Length	6000	60	240	240
Max. Length	6000	60	240	240
Min. No. of Series	1	100	100	100
Max. No. of Series	1	100	100	100
Forecast Horizon	12	12	12	12

Table 8: Characteristics of Generated Datasets from All DGPs

Characteristic	Value
No. of DGPs	4
Min. Length	600
Max. Length	600
Min. No. of Series	100
Max. No. of Series	100
Forecast Horizon	12

Table 9: Characteristics of Generated Datasets for the Group Feature Setup of the Chaotic Logistic Map DGP

with no seasonality or the seasonal naïve forecast for seasonal data. As seen in Equation 16, the denominator indicates this error from the relative benchmark where M denotes the seasonal period in case of seasonal data. According to Hyndman and Koehler (2006), MASE is the best performance metric available, being less susceptible to outliers and more interpretable than other error metrics.

Equations 15 and 16 only define the error calculation for a single series. Since our forecasting scenarios involve multiple series from many datasets, we consider the mean SMAPE and mean MASE measures to summarise the overall error distribution across all the series available.

5.3. Statistical Tests for Significance of the Differences

Our simulation study is designed in a manner such that the individual differences between the models are significant for every scenario. This is the objective behind performing every experiment on 100/1000 datasets, and then averaging across all these datasets to obtain the final results for every scenario. However, to show systematically that this is the case, we perform non-parametric Friedman rank-sum tests on few of the most important scenarios as explained in Section 6, to estimate the significance of differences. This is followed by Hochberg’s post hoc procedure to further analyse the differences relative to a control method, in particular the best method in every scenario (García et al., 2010). A significance level of $\alpha = 0.05$ is used for all the tests.

6. Results and Analysis

This section provides a detailed analysis of the results obtained for different experimental setups. Furthermore, we provide a comparison of the computational complexities of various forecasting variants employed in this study.

6.1. Comparison of Model Performance

The results from all the scenarios of all the DGPs are presented in Table 10 using both Mean SMAPE and Mean MASE values. In every column, the best-performing model under every DGP is indicated in boldface. Not all the models are relevant to all the experimental setups; hence the ‘-’ in some of the table cells. As mentioned before, since PR models are the global versions of AR models, we run only the AR models in the SS scenarios, as the AR and PR models become equivalent in case of just one series. Furthermore, we also present Table 11, which shows the percentage difference of every model from the best model in each scenario, computed according to Equation 18. In Equation 18, D_m is the percentage difference of the performance of model m , E_m is the error of model m and E_b is the error of the best model in the respective scenario. The error E in this case can be either the Mean SMAPE value or the Mean MASE value. Thus, according to Equation 18, the best performing model in every separate experimental setting has a ‘0’ in Table 11. Likewise, Table 11 helps identify how competitive every individual forecasting model is, with respect to the best performing model.

$$D_m = 100 * \frac{E_m - E_b}{E_b} \quad (18)$$

The analyses of different DGPs are presented separately. For every DGP, we discuss in detail the behaviour of the models with respect to the experimental scenarios indicated in Table 1. For the relevant models, we also indicate the number of lags used to train the model. For example, LGBM(3) refers to an LGBM model with an order of 3 lags. Although we conduct experiments for data availability for some of the DGPs, the numbers shown in Table 10 correspond only to the highest length/number of series in each scenario as per Table 8. For further results with all the error values corresponding to the different amounts of data available in every DGP, refer to Appendix A.

Model	SS		MS-Hom-Short		MS-Hom-Long		MS-Het	
	SMAPE	MASE	SMAPE	MASE	SMAPE	MASE	SMAPE	MASE
AR(3) DGP								
RNN(3)	18.04	0.55	18.12	0.61	21.37	0.54	21.78	0.86
RNN(10)	-	-	-	-	21.22	0.53	20.88	0.81
FFNN(3)	19.11	0.58	18.91	0.64	23.06	0.58	23.35	0.91
FFNN(10)	-	-	-	-	21.84	0.55	22.21	0.87
LGBM(3)	19.25	0.59	19.25	0.65	23.07	0.58	23.29	0.90
LGBM(10)	-	-	-	-	21.72	0.55	21.85	0.85
PR(3)	-	-	17.71	0.60	21.07	0.53	21.72	0.86
PR(10)	-	-	-	-	21.08	0.53	21.72	0.86
AR(2)	17.48	0.53	18.79	0.63	21.17	0.53	19.93	0.76
AR(3)	17.47	0.53	19.53	0.66	21.22	0.53	19.95	0.76
AR(10)	17.55	0.54	32.92	1.03	21.63	0.54	20.34	0.78
SAR(1) DGP								
RNN(12)	4.91	0.97	4.90	1.04	14.03	1.04	22.15	0.74
FFNN(12)	4.94	0.98	4.86	1.03	13.22	0.97	22.98	0.77
LGBM(12)	5.00	0.99	5.19	1.10	13.29	0.98	22.84	0.76
PR(12)	-	-	4.93	1.05	13.19	0.97	22.02	0.74
AR(12)	4.77	0.94	7.69	1.59	13.49	0.99	21.65	0.72
AR(3)	8.86	1.76	8.88	1.90	23.40	1.79	22.11	0.74
SAR(1)	4.75	0.94	4.90	1.04	13.18	0.97	21.20	0.70
Chaotic Logistic Map DGP								
RNN(15)	51.63	0.78	49.21	0.75	48.12	0.73	27.54	0.88
FFNN(15)	53.27	0.81	50.15	0.77	47.50	0.72	28.18	0.90
LGBM(15)	48.93	0.74	50.43	0.77	46.80	0.71	27.45	0.88
PR(15)	-	-	53.37	0.81	52.46	0.78	27.63	0.88
AR(15)	52.91	0.79	57.67	0.89	52.65	0.79	27.56	0.88
SETAR DGP								
RNN(15)	23.44	0.47	20.57	0.41	23.68	0.41	25.93	0.45
FFNN(15)	20.78	0.42	20.69	0.42	23.84	0.42	26.00	0.46
LGBM(15)	20.63	0.41	21.09	0.43	23.80	0.42	25.82	0.45
PR(15)	-	-	21.21	0.43	24.50	0.43	26.67	0.47
AR(15)	21.19	0.43	23.89	0.48	25.10	0.44	27.16	0.48
SETAR	20.52	0.41	22.26	0.44	25.61	0.44	29.10	0.51
Mackey-Glass Equation DGP								
RNN(15)	3.21	0.48	1.47	0.22	1.20	0.18	6.76	1.11
FFNN(15)	5.45	0.82	1.61	0.24	2.59	0.39	14.05	2.35
LGBM(15)	0.59	0.09	0.89	0.13	0.45	0.07	9.59	1.59
PR(15)	-	-	7.13	1.06	7.77	1.16	11.95	1.97
AR(15)	6.81	1.02	9.22	1.36	7.99	1.19	10.87	1.82

Table 10: Results from all Data Generating Processes

Model	SS		MS-Hom-Short		MS-Hom-Long		MS-Het	
	SMAPE	MASE	SMAPE	MASE	SMAPE	MASE	SMAPE	MASE
AR(3) DGP								
RNN(3)	3.26	3.77	2.32	1.67	1.42	1.89	9.28	13.16
RNN(10)	-	-	-	-	0.71	0.00	4.77	6.58
FFNN(3)	9.39	9.43	6.78	6.67	9.44	9.43	17.16	19.74
FFNN(10)	-	-	-	-	3.65	3.77	11.44	14.47
LGBM(3)	10.19	11.32	8.70	8.33	9.49	9.43	16.86	18.42
LGBM(10)	-	-	-	-	3.08	3.77	9.63	11.84
PR(3)	-	-	0.00	0.00	0.00	0.00	8.98	13.16
PR(10)	-	-	-	-	0.05	0.00	8.98	13.16
AR(2)	0.06	0.00	6.10	5.00	0.47	0.00	0.00	0.00
AR(3)	0.00	0.00	10.28	10.00	0.71	0.00	0.10	0.00
AR(10)	0.46	1.89	85.88	71.67	2.66	1.89	2.06	2.63
SAR(1) DGP								
RNN(12)	3.37	3.19	0.82	0.97	6.45	7.22	4.48	5.71
FFNN(12)	4.00	4.26	0.00	0.00	0.30	0.00	8.40	10.00
LGBM(12)	5.26	5.32	6.79	6.80	0.83	1.03	7.74	8.57
PR(12)	-	-	1.44	1.94	0.08	0.00	3.87	5.71
AR(12)	0.42	0.00	58.23	54.37	2.35	2.06	2.12	2.86
AR(3)	86.53	87.23	82.72	84.47	77.54	84.54	4.29	5.71
SAR(1)	0.00	0.00	0.82	0.97	0.00	0.00	0.00	0.00
Chaotic Logistic Map DGP								
RNN(15)	5.52	5.41	0.00	0.00	2.82	2.82	0.33	0.00
FFNN(15)	8.87	9.46	1.91	2.67	1.50	1.41	2.66	2.27
LGBM(15)	0.00	0.00	2.48	2.67	0.00	0.00	0.00	0.00
PR(15)	-	-	8.45	8.00	12.09	9.86	0.66	0.00
AR(15)	8.13	6.76	17.19	18.67	12.50	11.27	0.40	0.00
SETAR DGP								
RNN(15)	14.23	14.63	0.00	0.00	0.00	0.00	0.43	0.00
FFNN(15)	1.27	2.44	0.58	2.44	0.68	2.44	0.70	2.22
LGBM(15)	0.54	0.00	2.53	4.88	0.51	2.44	0.00	0.00
PR(15)	-	-	3.11	4.88	3.46	4.88	3.29	4.44
AR(15)	3.27	4.88	16.14	17.07	6.00	7.32	5.19	6.67
SETAR	0.00	0.00	8.22	7.32	8.15	7.32	12.70	13.33
Mackey-Glass Equation DGP								
RNN(15)	444.07	433.33	65.17	69.23	166.67	157.14	0.00	0.00
FFNN(15)	823.73	811.11	80.90	84.62	475.56	457.14	107.84	111.71
LGBM(15)	0.00	0.00	0.00	0.00	0.00	0.00	41.86	43.24
PR(15)	-	-	701.12	715.38	1626.67	1557.14	76.78	77.48
AR(15)	1054.24	1033.33	935.96	946.15	1675.56	1600.00	60.80	63.96

Table 11: Percentage Differences from the Best Model under each Experimental Scenario

Method	p_{Hoch}
AR(3)	-
AR(2)	0.53
AR(10)	0.04
RNN(3)	6.67×10^{-8}
FFNN(3)	2.17×10^{-19}
LGBM(3)	3.39×10^{-27}

Table 12: Results of Hochberg’s post-hoc procedure for the AR(3) DGP SS scenario, by using the AR(3) model as the control method. The adjusted p -values indicate that the AR(2) model is not significantly worse from the AR(3) model in this case. All the other models perform significantly worse from the best method AR(3).

6.1.1. AR(3) Data Generating Process

Figure 5 illustrates how the performance of the forecasting models under the AR(3) DGP setting evolve with increasing lengths and number of series. In Table 10, under the SS scenario of the AR(3) DGP, in between the three AR processes, AR(3) is better which is not surprising as this is the model of the DGP. When comparing with all the other models as well, the AR(3) model performs the best, with the AR(2) being the second and the AR(10) the third, with respect to mean SMAPE. The true DGP AR(3) is in fact a subclass of the AR(10) forecast model, in which case the training process of the AR(10) model resolves to identifying that the coefficients beyond the third lag are close to 0. According to Table 11 also, it is clear that in the SS setting, AR(2) and AR(10) are the closest to the true model, whereas among the non-linear models, RNN(3) is the closest to the best performing model AR(3). However, when looking at the SS scenario in Figure 5, we can see that at the beginning lengths, the AR(2) model is better than the AR(3). It is after the series reaches adequate length that the AR(3) model starts to outperform the AR(2) model. This observation complies with the findings of [Kunst \(2008\)](#) that an AR(2) can be better than an AR(3) if there are not enough data for the model to fit all parameters reliably. A similar situation is observed among the AR(10) model and the other non-linear models RNN(3), FFNN(3) and LGBM(3). Due to the high amount of coefficients to be trained in the AR(10) model, the small lengths of the series are not sufficient to capture the underlying AR(3) process clearly. For the SS scenario of the AR(3) DGP, the Friedman test of statistical significance gives an overall p -value of 1.21×10^{-10} in terms of the mean SMAPE values. This indicates that the differences in between the models in this case are statistically highly significant. Hochberg’s post-hoc procedure on these results by using the best model AR(3) as the control method, gives the adjusted p -values indicated in Table 12.

When moving to the multiple series context, the local AR model, which learns only from the current series, becomes clearly worse in the MS-Hom-Short scenario as the lengths of the individual series are much shorter (18 data points). Among the AR models as well, we can see how the performance gets worse with the increased number of coefficients, with the AR(10) being the worst and the AR(3) being the second worst. The PR(3) model performs best as shown in the MS-Hom-Short columns. This outcome is apparent given that the underlying DGP is an AR(3), so that a linear model of the corresponding order performs competitively. As shown in both Table 10 and 11, the RNN(3) model is the next best to the PR(3) in the MS-Hom-Short setting. The RNN(3) model in this case acts as a more complex model to the PR(3), with its non-linear modelling capability, yet without increasing the actual model order. Furthermore, in a very short length scenario like this, it is evident how the global models such as PR(3) and RNN(3) which learn from all the series can be better than the local models, even the one closest to the true DGP which is AR(3). The line plots of Figure 5 corresponding to the MS-Hom-Short scenario reaffirm the findings of [Kunst \(2008\)](#) that the AR(2) can outperform the AR(3) at short lengths of the series. In the MS-Hom-Short scenario where the length of all the series is 18, this is seen across all the dataset sizes. In fact, at the beginning lengths, the AR(2) is the best model and gradually the PR(3) starts to outperform as the number of series in the dataset increases.

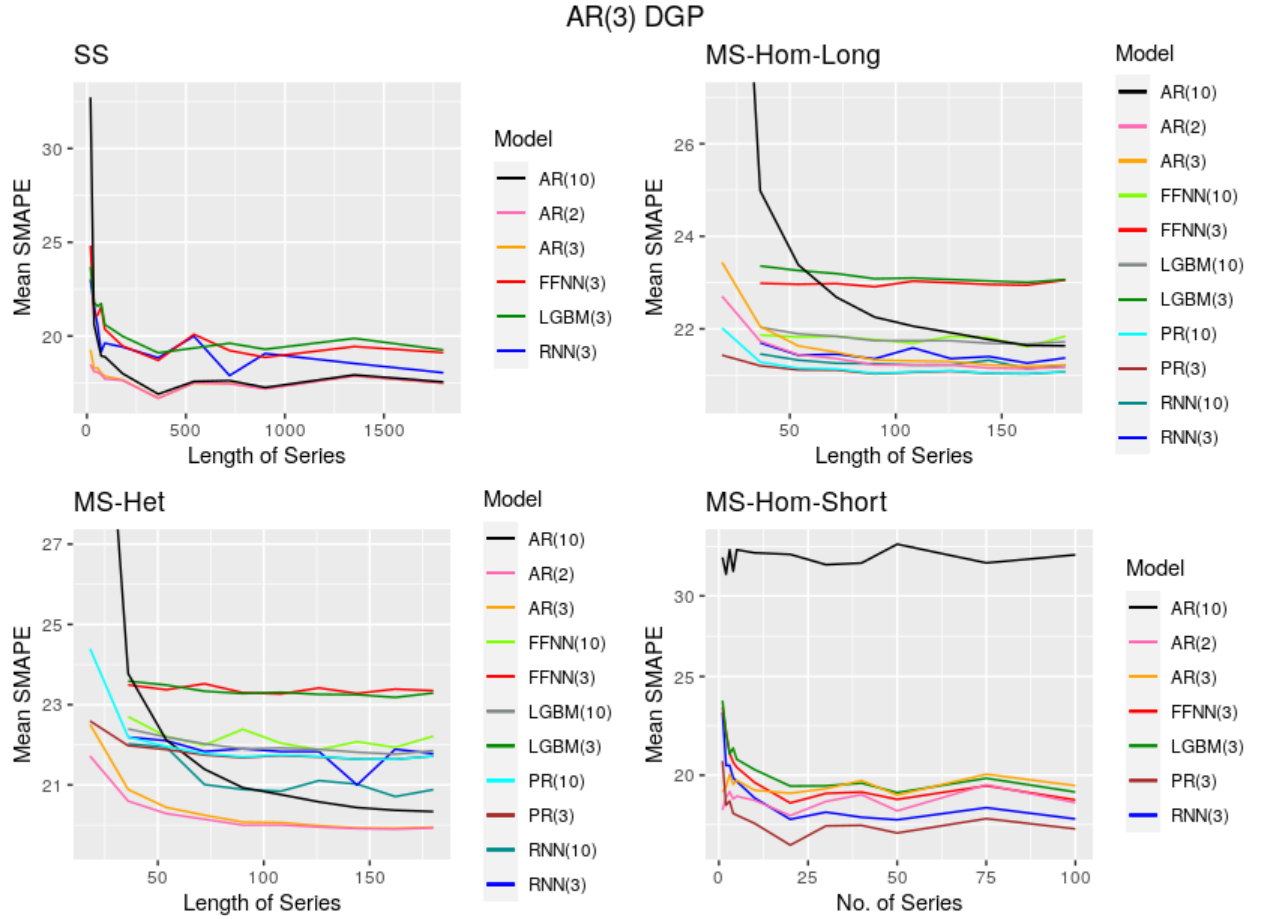


Figure 5: Visualisation of the Change of Errors of the Models Across Different Amounts of Data in the AR(3) DGP Scenarios

On the other hand, the AR(10) remains the worst performing model across all dataset sizes.

It is due to the data shortage in the MS-Hom-Short scenario that we experiment with varying lengths of the series in the MS-Hom-Long scenario while keeping the number of series constant. The idea is to increase the lengths in a multi-series setting, so that the local models which learn from individual series can again become competitive against the global models which learn across series. Furthermore, since we have sufficient data points in the MS-Hom-Long scenario, we also run the PR, RNN, LGBM and FFNN models with both 3 and 10 lags. As seen in the MS-Hom-Long columns of Table 10 and 11, the difference of the performance between the two models PR(3) and PR(10) is quite small. Similar to the MS-Hom-Short scenario, the PR models still remain the best out of all the models in the MS-Hom-Long scenario, in terms of Mean SMAPE. This is again due to the underlying linearity of the data generated by the AR(3) DGP, that the linear PR models outperform all the others. However, it is also worth noting that the AR(2) and AR(3) models in the MS-Hom-Long scenario are much closer in performance to the PR models. This observation can be attributed to the increased lengths of the series (180 points) in the MS-Hom-Long scenario which constitute enough data in one series itself for the local models to train properly. Yet, the PR model outperforms in terms of Mean SMAPE since the series are all homogeneous and the global, linear PR model learns better across the series. As seen in Table 10, the lag 10 models all outperform their lag 3 variants for the complex models, which explains that adding more memory/complexity to the models, supported by the increased lengths of the series helps the complex models learn better. In fact, with respect to mean MASE, RNN(10) demonstrates an equivalent performance to that of the best models PR(3), PR(10). In terms of Mean SMAPE, the RNN(10) model demonstrates the same result as the AR(3) model which is in fact the true DGP. It is also worth noting that both RNN variants are better than the AR(10) model in terms of Mean SMAPE values. This indicates that 180 is still not enough length for the AR(10) model to identify the underlying AR(3) pattern, since on the other hand in the SS setting with much longer lengths, the AR(10) outperforms the RNN. Looking at the MS-Hom-Long setting in Figure 5 which shows the errors evolving through increasing series lengths, we can see that AR(10) is in fact the worst performing model in the beginning lengths similar to the observations from the MS-Hom-Short scenario. It is as the lengths increase that the AR(10) starts to outperform the FFNN and LGBM models.

Moving on to the heterogeneous series scenario, the AR(2) and AR(3) models again emerge as the best models with the AR(10) being the third. This is intelligible, since the underlying patterns are now more complex due to the induced heterogeneity among the series. The dataset can be seen as no longer holding a simple linear pattern, but a combination of many of them. A global model trained over all the series builds one function over all the different individual patterns. Therefore, the local AR models built per every series which do not account for cross-series information, outperform all the global models. Nevertheless, among the global models, the RNN(10) model performs better than the linear PR models since the inherent complex, non-linear modelling capacity of the RNN model can account for the heterogeneity among the series to a certain extent. Furthermore, looking at Table 11, it is clear that the percentage difference between the best performing local models and the RNN(10) is very small (4.77% in terms of Mean SMAPE) compared to the differences of other models, which again emphasizes the competitive performance of the RNN(10) in this case. Also, similar to the MS-Hom-Long scenario in this setting too, increasing the model order of the non-linear models to improve the complexity helps since the lag 10 variants outperform the lag 3 variants. It is also important to observe that the MASE values of all the non-linear models in all the scenarios are less than 1, indicating that their performance is better than the performance of the naïve forecasts in-sample. Looking at the error visualization of the models across lengths of the MS-Het scenario in Figure 5, we can see that the AR(10), although it outperforms all the global models at the maximum length, performs the worst in the beginning lengths as expected. Moreover, the PR(10) performs better than its corresponding local model AR(10) at the beginning lengths. Similarly, both RNN models perform better than AR(10) at shorter lengths. This observation demonstrates that although local models can be competitive in a heterogeneous series setting like this, they require sufficient lengths in the series for such good performance. If the individual series are too short for the local models, having global models,

Method	p_{Hoch}
AR(2)	-
AR(3)	0.51
AR(10)	3.73×10^{-22}
PR(3)	$< 10^{-30}$
PR(10)	$< 10^{-30}$
RNN(3)	$< 10^{-30}$
RNN(10)	$< 10^{-30}$
FFNN(3)	$< 10^{-30}$
FFNN(10)	$< 10^{-30}$
LGBM(3)	$< 10^{-30}$
LGBM(10)	$< 10^{-30}$

Table 13: Results of Hochberg’s post-hoc procedure for the AR(3) DGP MS-Het scenario, by using AR(2) model as the control method. The adjusted p -values indicate that the AR(3) model is not significantly worse from the AR(2) model in this case. All the other models perform highly significantly worse from the best method AR(2).

especially complex non-linear ones such as RNNs in a heterogeneous setting like this, which learn across all the short series together can be quite competitive. Friedman test of statistical significance for the MS-Het scenario gives an overall p -value of 2.59×10^{-10} in terms of the mean SMAPE values which means that the differences are statistically highly significant. Hochberg’s post-hoc procedure by using AR(2) as the control method, gives the adjusted p -values shown in Table 13.

According to Figure 5, we can see the effect from increasing the amounts of data in the datasets for the different experimental scenarios of the AR(3) DGP. From this visualisation, it is evident that the accuracies of all the models in general improve by increasing the length of the time series or the number of time series, except for the local models in the MS-Hom-Short scenario where we only increase the number of series in the dataset.

6.1.2. SAR(1) Data Generating Process

As seen in Table 10 for the SAR(1) DGP, the SAR(1) model is the best on the SS scenario, which is again obvious given that SAR(1) is the closest to the true DGP. On the other hand, the AR(3) model which is clearly a misspecified model with respect to the SAR(1), is the worst irrespective of the huge length of the series in the SS setting. The AR(12) in the SS setting is quite close to the SAR(1) and equivalent in performance to SAR(1) in terms of Mean MASE. This is also more clearly captured in the SS column of Table 11. Unlike with AR(3), AR(12) is a superclass of the true DGP SAR(1), where only the 12th coefficient needs to be significant. Thus, the training process of the AR(12) model under the SAR(1) DGP can learn this with sufficient length in the series. In the MS-Hom-Short scenario with the same data, the AR(3) model still remains the worst performing model, following the understanding from the SS scenario. However, the AR(12) has also become the second worst performing model in the MS-Hom-Short setting. Among the local models, this observation is comprehensible due to the heavy complexity of the AR(12) model compared to the SAR(1) model which has just one coefficient and the short lengths of the available series (24 points) associated with the MS-Hom-Short scenario. The model closest to the true DGP which is SAR(1) shows the same performance as the RNN(12) and is the second best model. It is an important observation here that the FFNN outperforms the SAR(1) model which is the true DGP, although SAR(1) has just one coefficient to be trained, for which even the short lengths of the series in the MS-Hom-Short setting are adequate. This shows the competence of the models that learn across series in such homogeneous contexts. The PR(12) model in the MS-Hom-Short scenario closely follows the SAR(1) and RNN(12) models.

When the lengths of the series are increased as per the results of the MS-Hom-Long scenario, once again the SAR(1) model surpasses all the other models. However, the PR(12) model is almost the same as the SAR(1) model with the FFNN being the next following the PR(12). All three of them are

equivalent in performance with respect to the Mean MASE values. In this MS-Hom-Long scenario, it is evident that the unnecessary complexity of the models lead to poor performance, since the underlying DGP is an SAR(1) with just one coefficient. For example, the AR(12) model which is built per every series is a quite complex model with 12 coefficients for every individual series, with just one of them being actually necessary to model the series perfectly. Similarly, the RNN(12), although built across series, still holds inherent complexity in the model. This explains their poor performance on the MS-Hom-Long scenario. The PR(12) on the other hand, although it has 12 coefficients, has just sufficient complexity with its linear modelling to perform competitively. With the AR(3), it is apparent how too much simplicity can also result in impaired performance of the misspecified models. In the MS-Het scenario, the SAR(1) model again becomes the best, complying with the observation in the AR(3) DGP that building one model per every series can be promising in this kind of a heterogeneous scenario. The second best model in this case is the AR(12) model, although it shows poor performance on the previously described homogeneous series scenarios. This is again due to the complexity of the data in the heterogeneous setting, that the complex, local AR(12) model built per every series becomes quite competitive compared to other global models. Among the global models, the PR(12) is the best. The RNN(12) is quite close and is exactly equal in performance to PR(12) with respect to Mean MASE. This indicates that, although the RNN is a competitive model due to its complexity in the heterogeneous setting, under the SAR(1) DGP with just one coefficient for every series, the RNN's high complexity may be unnecessary. Surprisingly, the misspecified AR(3) model outperforms all the non-linear global models in the MS-Het scenario. Theoretically this is highly unlikely for AR(3) even with the heterogeneous series, since it should not be able to capture the pattern in a single SAR(1) generated series. However, this result is intelligible given that in the MS-Het setting we generate series by randomly picking a coefficient from $U(-0.5, 0.5)$ to induce heterogeneity. Some of these series in the MS-Het scenario may end up getting non-significant 12th lags depending on how big the coefficient is. Consequently, the AR(3) model may no longer be a misspecified model for the series in this MS-Het scenario, and thus its competitive performance. On the other hand in the MS-Hom-Long setting, the underlying SAR(1) model used has a coefficient of 0.85 as mentioned in Section 3, which is chosen intentionally to create series with longer memory, and thus the inferior performance of AR(3) in that scenario.

In the SAR(1) DGP too, the observations related to data availability are the same as for the AR(3) DGP, i.e., the performance of all the models improves in general as the size of the dataset increases, although not quite consistent across the individual lengths and number of series in some scenarios. As expected, this drop in errors does not hold for the case with local models on the MS-Hom-Short scenario. This is demonstrated by the line plots in Figure 6. For mean SMAPE and mean MASE values corresponding to all the data availability experiments, refer to [Appendix A.2](#).

6.1.3. Chaotic Logistic Map Data Generating Process

As shown in Table 10, the non-linearity of the patterns generated by the Chaotic Logistic Map DGP are perceived by the non-linear forecasting models outperforming the linear ones in all the different experimental scenarios. In Table 10, for the SS scenario, even though there is only one DGP with the same coefficients, due to the complexity inherent in the DGP, the complex patterns produced are not captured well by the linear model AR(15). The LGBM(15) is the best model on the SS scenario. On the other hand on the MS-Hom-Short scenario, as indicated in Table 10, the RNN(15) is the best model with the FFNN(15) and the LGBM(15) being quite close. Once again, the lengths of the short series in the MS-Hom-Short scenario are not sufficient for the AR(15) model to properly learn all its 15 coefficients. However, the PR(15) model, although linear in nature, as it learns across series it performs better than the AR(15) model in the MS-Hom-Short scenario, due to the underlying homogeneity of the series. However, since the individual series hold complex patterns, the linear PR is still not sufficient to surpass the complex global models in the MS-Hom-Short scenario. For the MS-Hom-Short scenario of the Chaotic Logistic Map DGP, the Friedman test of statistical significance gives an overall p -value of 3.12×10^{-10} indicating the significance of the differences between the models. Hochberg's post-hoc procedure for this scenario gives the adjusted p -values shown in Table 14, by using the best method

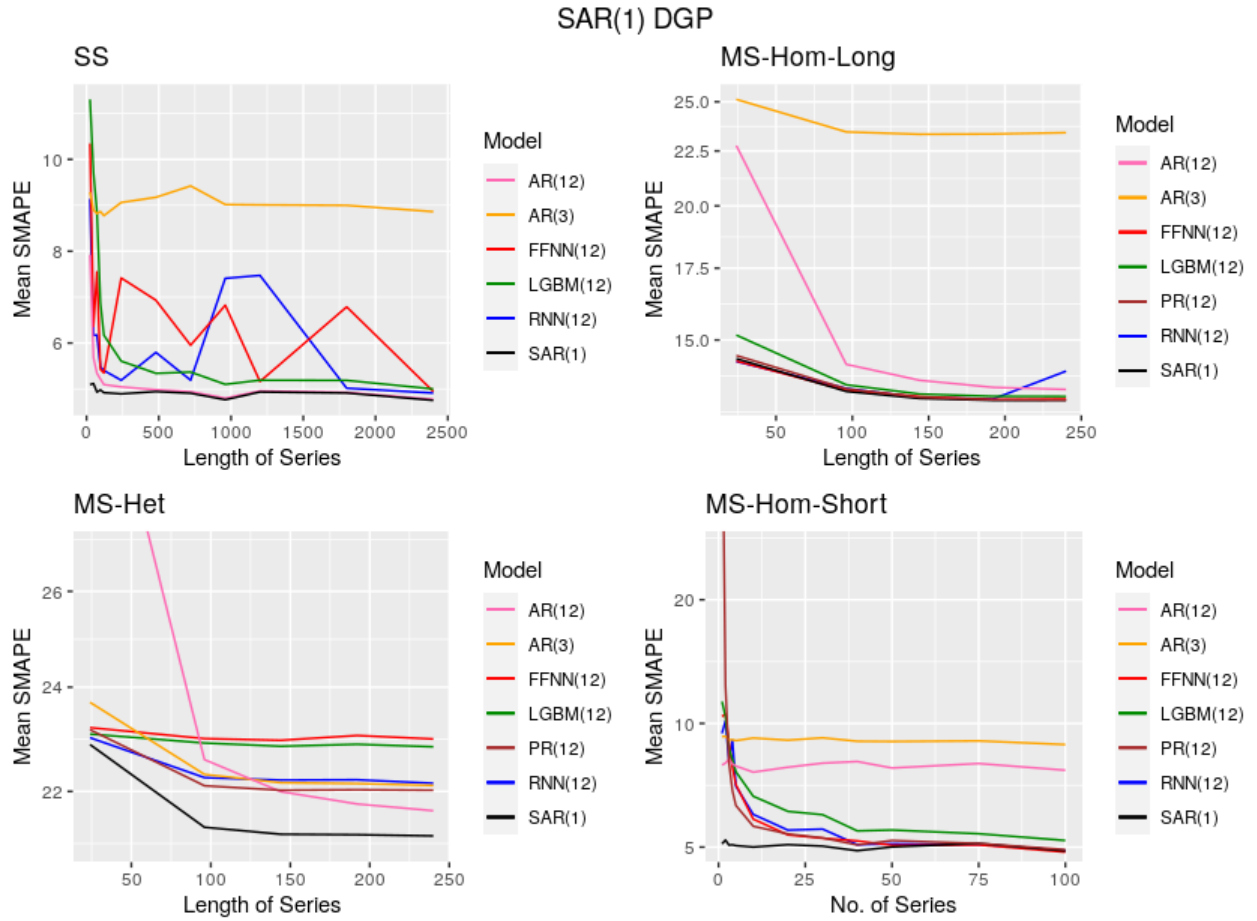


Figure 6: Visualisation of the Change of Errors of the Models Across Different Amounts of Data in the SAR(1) DGP Scenarios

Method	p_{Hoch}
RNN(15)	-
LGBM(15)	6.08×10^{-3}
FFNN(15)	6.08×10^{-3}
PR(15)	$< 10^{-30}$
AR(15)	$< 10^{-30}$

Table 14: Results of Hochberg’s post-hoc procedure for the Chaotic Logistic Map DGP MS-Hom-Short scenario, by using RNN(15) model as the control method. The adjusted p -values indicate that all the other models are significantly worse than the RNN(15) model in this case.

Method	p_{Hoch}
LGBM(15)	-
FFNN(15)	$< 10^{-30}$
RNN(15)	$< 10^{-30}$
PR(15)	$< 10^{-30}$
AR(15)	$< 10^{-30}$

Table 15: Results of Hochberg’s post-hoc procedure for the Chaotic Logistic Map DGP MS-Hom-Long scenario, by using the LGBM(15) model as the control method. The adjusted p -values indicate that all the other models are significantly worse from the LGBM(15) model in this case.

RNN(15) as the control method.

With the varying length experiments, as shown on the MS-Hom-Long columns of Table 10, still the non-linear complex models RNN(15), FFNN(15), and LGBM(15) win over the linear models AR(15) and PR(15), while the LGBM(15) is the best. However, similar to the previous DGPs, in this scenario too, the drop of the errors in the AR model due to the length increase is notable. The lengths of the individual series in this case seem sufficient for the AR(15) to learn competitively, despite its complexity. Yet, due to the homogeneity of the multiple series, the PR(15) which learns across series is ahead of the AR(15) in terms of the performance. For this scenario, the Friedman test of statistical significance gives an overall p -value of $< 10^{-30}$. Thus, similar to previous scenarios, this too demonstrates high significance of the performance differences between the models. Hochberg’s post-hoc process on these results by using LGBM(15) as the control method, gives the adjusted p -values which are shown in Table 15.

In the MS-Het scenario, the SMAPE values of all the models have dropped substantially compared to all the other scenarios. This is due to the fact that in all the other homogeneous scenarios of this DGP, we specifically select the coefficients mentioned in Section 3.2 such that the generated patterns are equally hard to be captured by all the models. However, in the heterogeneous scenario, since the coefficients are generated randomly for the different series, there is no such guarantee regarding the coefficients. Even though, the patterns become relatively easy to be modelled by all the forecasting models in the heterogeneous scenario with respect to the mean SMAPE values, still the non-linear global models outperform the two linear AR and PR models. This observation reiterates our understanding that the Chaotic Logistic Map is a complex non-linear DGP whose patterns are only correctly captured by complex forecasting models. Furthermore, similar to the previous DGPs, the AR(15) outperforms the PR(15) in the MS-Het scenario of the Chaotic Logistic Map DGP. This is explained by the heterogeneity of the series, where a local model built on every series can be better than a linear model which learns across series.

As with the previous DGPs, with the Chaotic Logistic Map DGP too, we can observe that the models improve with increased amounts of data in general. The visualisation of these data availability experiments is depicted in Figure 7. Based on the conclusions obtained regarding data availability for

forecasting from all the experimental scenarios explained thus far, we eliminate the data availability experiments from the rest of the experimental setups explained next. The idea is that, since the performance of all the models improve with either increasing lengths or the number of series, for the remaining experiments, one specific length and a number of series are used.

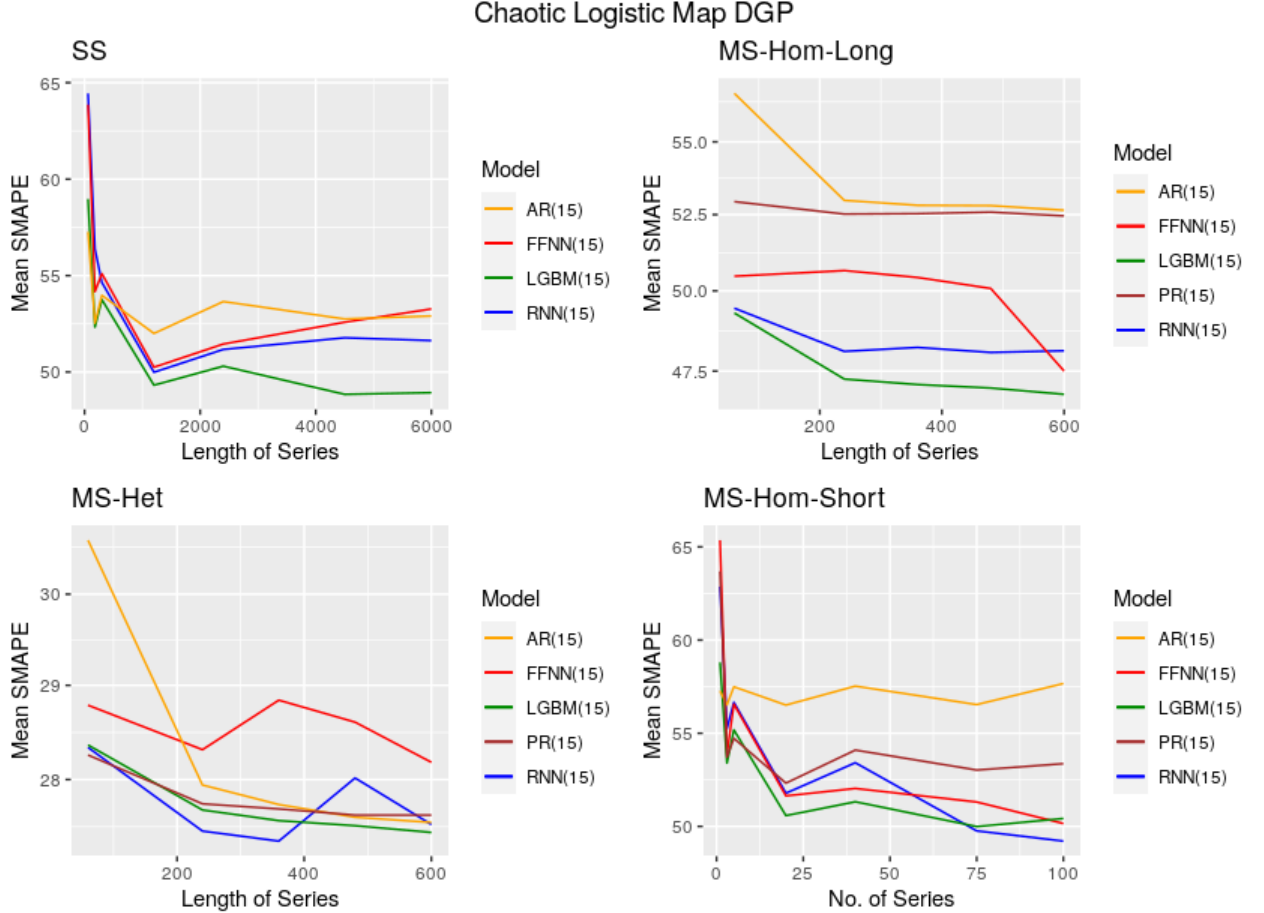


Figure 7: Visualisation of the Change of Errors of the Models Across Different Amounts of Data in the Chaotic Logistic Map DGP Scenarios

6.1.4. SETAR Data Generating Process

For the SS scenario results shown in the first two columns under the SETAR DGP of Table 10, the length of the series used is 6000. The best model under the SS scenario in this case is the true model which is SETAR. It seems that the lengths of the series in the SS setting are sufficient for the local non-linear SETAR model to properly capture the underlying patterns in the series. Once again, the complexity of the DGP is visible by the non-linear models FFNN(15) and LGBM(15) outperforming the linear AR(15) model. However, the RNN(15) becomes the worst model in this scenario. SETAR models are regime switching models meaning that the coefficients of the underlying AR model changes from time to time even within the same series. This is the origin of the non-linearity in the SETAR DGPs. On the other hand, the nature of the RNN models is that they have a long-term memory especially with the LSTM cells on such long series with 6000 points. Nevertheless, on a SETAR generated series, such long memories are not quite useful due to regime switching. Apart from the SS scenario, the SETAR DGP results are quite similar to those from the Chaotic Logistic Map DGP.

For the MS-Hom-Short experiment, the length of every individual series is 60 with 100 series in the dataset (corresponding to the 6000 data points in the SS scenario). According to the MS-Hom-Short columns of Table 10, in the MS-Hom-Short scenario of the SETAR DGP, the RNN(15) is the best model followed by the FFNN(15) and the LGBM(15). Similar to the previous DGPs, the errors of the local AR and SETAR models increase due to short lengths of the series in the MS-Hom-Short scenario. Moreover, although the global PR is better than the local AR and SETAR models under the MS-Hom-Short setting due to the homogeneity of the series, the linear modelling of the PR is not adequate to capture the complex patterns produced by the SETAR DGP for the individual series.

In the MS-Hom-Long scenario of the SETAR DGP, we fix the lengths of the series to 240, and the number of series to 100. Therefore, the MS-Hom-Long scenario in this case acts as an increased length version of the MS-Hom-Short scenario. The same length of 240 is used for the MS-Het scenario too with a set of 100 series in one dataset. As seen in Table 10, the non-linear global models surpass the linear AR, SETAR and PR models in both the MS-Hom-Long and MS-Het scenarios. The result of the MS-Hom-Long scenario is just the same as the MS-Hom-Short scenario, except that the AR and the PR models are closer in performance in the MS-Hom-Long setting, due to the increased lengths of the series that are helpful for the AR model. However, for the SETAR model the increased lengths still do not seem to be sufficient to capture the non-linear patterns of the series properly. The AR(15) model seems to learn some patterns better than at least the SETAR model with the increased lengths in the MS-Hom-Long scenario. Yet, they are both inferior in performance to the PR model which learns across series in this homogeneous case, although the individual series hold complex non-linear patterns. However, in the heterogeneous scenario, different from the previous DGPs, the PR model performs better than both the AR and SETAR models. For the AR models, this can be explained by the regime-switching nature of the series generated by the SETAR DGP. Apart from the different patterns among the series, the pattern changes within the series itself. Due to this reason, one AR model trained for the whole series is not the ideal model for this scenario, although it performs quite well under the heterogeneous settings of the other DGPs. Furthermore, although the true model is the best under the heterogeneous settings of the DGPs explained previously, it is not the case with the SETAR DGP. The SETAR model in the heterogeneous case is still the worst performing model due to the insufficient lengths of the series. Also, looking at Table 11, we can see that in the MS-Hom-Long scenario, the difference of the percentage differences among the local and global models is smaller than in the MS-Het scenario. Furthermore, the percentage difference of the SETAR model has increased substantially from 8.15% to 12.70% in terms of Mean SMAPE. This can be explained by the involvement of random coefficients in the MS-Het scenario which makes it difficult for all forecasting techniques to model the series in the MS-Het context in general.

6.1.5. Mackey-Glass Data Generating Process

The number and the lengths of the series in all the scenarios of the Mackey-Glass DGP are the same as in the SETAR DGP. Moreover, the observations from the Mackey-Glass DGP too are very similar to those from the SETAR and Chaotic Logistic Map DGPs. The Mackey-Glass Equation is used in the study to restate the benefit of non-linear forecasting models when applied on datasets having complex, non-linear characteristics. This is supplemented by the results in Table 10. The non-linear models RNN(15), FFNN(15), and LGBM(15) outperform the linear models in most of the scenarios. The LGBM(15) model is remarkably better than all the other models under the SS, MS-Hom-Short and MS-Hom-Long scenarios. This is also confirmed by the Friedman test of statistical significance for the SS scenario, which gives an overall p -value of 1.08×10^{-10} , suggesting that the results are statistically highly significant. Further tests with Hochberg’s post-hoc procedure by using LGBM(15) as the control method, give the adjusted p -values shown in Table 16. Similar to the previous DGPs, the PR model is better than the AR model in both the MS-Hom-Short and MS-Hom-Long scenarios, due to the homogeneity among the series. The lengths increase in the MS-Hom-Long scenario has caused the AR model to come quite close in performance to the PR model in the MS-Hom-Long scenario. The complexity of the datasets in the MS-Het scenario is evident by the substantial increase of the SMAPE values in all the models. Furthermore, complying with our previous observations, in the

Method	p_{Hoch}
LGBM(15)	-
RNN(15)	1.08×10^{-12}
FFNN(15)	1.36×10^{-30}
AR(15)	$< 10^{-30}$

Table 16: Results of Hochberg’s post-hoc procedure for the Mackey-Glass DGP, SS scenario, by using the best method LGBM(15) as the control method. The adjusted p -values indicate that all the other models are significantly worse than the LGBM(15) model in this case.

Method	p_{Hoch}
RNN(15)	-
LGBM(15)	1.10×10^{-4}
AR(15)	1.48×10^{-16}
PR(15)	$< 10^{-30}$
FFNN(15)	$< 10^{-30}$

Table 17: Results of Hochberg’s post-hoc procedure for the Mackey-Glass DGP, MS-Het scenario, by using the best method RNN(15) as the control method. The adjusted p -values indicate that all the other models are significantly worse than the RNN(15) model in this case.

heterogeneous scenario of the Mackey-Glass DGP too, the local AR model appears to be better than the global PR model, due to the inherent heterogeneity of the datasets. For the heterogeneous case, the Friedman test gives an overall p -value of 1.74×10^{-10} , once again indicating the high significance of the performance differences. Hochberg’s post-hoc process for the heterogeneous scenario gives the p -values shown in Table 17.

6.1.6. Results of the Group Feature Experiments

The results from the Group Feature setup experiments performed on the Chaotic Logistic Map DGP are presented in Table 18. For this we use 100 datasets, each having series of length 240. The horizontal line in Table 18 separates the GFM.GroupFeature setup results with their corresponding GFM.All results along with the local AR model results. In this scenario, each dataset has series generated from four different sets of coefficients. The “GroupFeature” suffix indicates that the GFM.GroupFeature training paradigm explained in Section 2.5 is used on the respective models to increase the complexity of the base models. As seen in Table 18, the GFM.GroupFeature setup improves the accuracy of the GFM.All setup in all techniques except the PR model where the SMAPE value remains constant. Especially in the case of the FFNN, the group feature inclusion results in the base model improving beyond the PR models. All the non-linear GroupFeature models hold a better standing over the linear models in this scenario, while the RNN(15)-Group performs the best.

The Friedman test of statistical significance for the Group Feature scenario gives an overall p -value of 2.08×10^{-10} , expressing that the differences are statistically highly significant. Further tests with Hochberg’s post-hoc procedure, where the RNN(15)-Group is considered the control method, give the adjusted p -values shown in Table 19.

6.2. Comparison of Computational Complexities

The computing resources for the experiments are allocated from the Massive High Performance Computing Facility (eResearch Centre., 2019). Thus, the experiments are run on an allocation having an Intel Xeon E5-2680 v3 processor (2.50 GHz), 6 CPU cores with 2 threads per core and a main memory of 64GB. Under these experimental settings, we provide a comparison of the computational times of the different forecasting models. For this, we select the MS-Hom-Long scenario of the SETAR

Model	SMAPE	MASE
RNN(15)	38.27	0.87
FFNN(15)	39.13	0.90
LGBM(15)	37.39	0.86
PR(15)	38.89	0.87
AR(15)	39.31	0.88
RNN(15)-Group	36.68	0.84
FFNN(15)-Group	38.40	0.88
LGBM(15)-Group	37.05	0.85
PR(15)-Group	38.89	0.87

Table 18: Mean SMAPE and Mean MASE values for the GFM.GroupFeature Setup

Method	p_{Hoch}
RNN(15)-Group	-
LGBM(15)-Group	0.22
LGBM(15)	3.24×10^{-5}
RNN(15)	1.16×10^{-16}
FFNN(15)-Group	1.23×10^{-24}
FFNN(15)	$< 10^{-30}$
PR(15)-Group	$< 10^{-30}$
PR(15)	$< 10^{-30}$
AR(15)	$< 10^{-30}$

Table 19: Results of Hochberg’s post-hoc procedure for the Chaotic Logistic Map DGP, Group Feature scenario, by using the best method RNN(15)-Group as the control method. The adjusted p -values indicate that all the models, except LGBM(15)-Group are significantly worse than the RNN(15)-Group model in this case.

Model	Data Preprocessing	Model Training & Testing	Total
RNN(15)	5.36	10788.62	10793.98
FFNN(15)	5.36	649.73	655.09
LGBM(15)	5.36	4.58	9.94
AR(15)	-	111.08	111.08
SETAR	-	3.03	3.03
PR(15)	0.05	0.40	0.45

Table 20: Computational Times Comparison of the Forecasting Models (in seconds)

DGP which involves 100 datasets of 100 series in each of them with a length of 240 per series. In Table 20, we record the time taken for one of the 100 datasets with a breakdown on the individual durations for the different steps such as data preprocessing and model training & testing. Data preprocessing is not relevant for the AR(15) and SETAR models. Since RNN, FFNN, and LGBM all use the data preprocessed in the same manner, their data preprocessing times are the same. As observed from Table 20, the NN-based techniques spend comparatively higher computational times, with the RNN taking the highest and the FFNN the second highest time. The PR models in general are the most efficient out of all the models used in this study, while the SETAR and the LGBM models are the second and third most efficient models respectively. Compared to LGBM and PR, which are global models, the local AR model in this case with its 15 coefficients also takes a considerable amount of time due to the fact that it builds many models, one per each series.

6.3. Overall Summary of Results

In this section, we provide a summary for the overall results obtained. With respect to the data availability experiments, we can confirm the expected behaviour that the performance of all models, both local and global variants, improve as the individual series get longer. Also as expected, this is not the case with local models when we increase the number of series in the dataset, while keeping the lengths constant. Considering the experiments related to single and multiple series, although the error values are not exactly the same, all global model accuracies are roughly equivalent in the SS and MS-Hom-Short scenario. This indicates that for global models it does not make much difference whether the data remains on one long series or spread across multiple different series. However, due to the diversity of the experiments involved and the different complexities of the model architectures picked by the automated hyperparameter tuning technique applied for every individual scenario, there are some exceptions to this conclusion, such as the FFNN in the Mackey-Glass Equations DGP and the RNN in the SETAR DGP. The mean MASE values for the SS and the MS-Hom-Short scenarios are not comparable here, since the data points considered for the in-sample naïve error used in the denominator of the MASE metric differ in the two contexts. As mentioned before, the local AR models clearly become worse when moving to the MS-Hom-Short context, since less data is used for the model training then. Again, there are exceptions to this conclusion such as the SAR(1) forecast model in the SAR(1) DGP case. With its single coefficient, the SAR(1) model can be trained well with minimal training data. Along the same lines, although intended to be sufficient, the lengths in the MS-Hom-Long settings can still be inadequate for certain local models depending on the underlying DGPs. An example of this is the MS-Hom-Long setting of the SETAR DGP where the SETAR model performs the worst.

From Tables 10 and 11, we can see that with the existence of just a single series having adequate length, with either complex or simple patterns, the local forecast model closest to the true DGP if known, can win over all the other models, both local and global. However, when moving into the MS-Hom-Short scenarios, it is evident that this can happen only if the individual series are long enough for the local models to train well. This depends on the lengths of the series as well as the complexity of the local model in terms of the number of coefficients. If the lengths of series are not sufficient in

multiple series scenarios, the power of global models which learn across series come into play. With these global models as well, the ones closest to the true underlying DGP can win, such as the PR(3) in the MS-Hom-Short and MS-Hom-Long scenarios of the AR(3) DGP. On the other hand, the more complex the patterns in the individual series, the more complex global models can win, as seen with the MS-Hom-Short and MS-Hom-Long scenarios of the Chaotic Logistic Map DGP, SETAR DGP and Mackey-Glass Equation DGP in this study. Even if the individual series lengths are sufficient for local models, if the series in the dataset are all homogeneous, the global models which learn across series are still competitive over local ones which learn only from a single series. However, it still holds with these increased lengths that the more complex the patterns in the individual series, the more complex global models can win and the more simpler the patterns, the simple global models such as PR can win overall. Furthermore, even on series having complex patterns with adequate lengths, if the series are all homogeneous, the simple linear global models can outperform the local models as seen under the MS-Hom-Long scenarios of the Chaotic Logistic Map, SETAR and Mackey-Glass-Equation DGPs. When moving into the heterogeneous series settings, again the local models become competitive especially over the simple, linear global models when the individual series contain sufficient lengths, as observed in the heterogeneous scenarios of all the DGPs except SETAR. Once again, the potential of the global models come into play in the heterogeneous series settings, when the series lengths are short. However, unlike in the homogeneous settings, with the heterogeneous scenarios, the complex, non-linear global models are very competitive over simple, linear global models, with both simple and complex patterns in the individual series, as seen in the AR(3), Chaotic Logistic Map, SETAR and Mackey-Glass Equation DGPs. Apart from that, as seen in the AR(3) DGP case, for complex, non-linear global models, adding more memory/lags can help the models learn the patterns better. Furthermore, as shown in Table 18, under the Group Feature scenario, among the GFM.All setup models, the LGBM achieves the best results. However, adding external information to the GFM.All models regarding the existence of pre-known clusters within the data can further improve the model performance. This is confirmed by almost all the GFM.GroupFeature models outperforming their corresponding GFM.All setup models. In fact, the RNN.GroupFeature model becomes the best under these circumstances. Therefore, this attests our understanding that the GroupFeature setup can add more complexity to the base global model.

Thus, the linear models such as PR, AR work best with known linear patterns in the data. On the other hand, non-linear models such as LGBM, RNN are more general in that they can perform reasonably well irrespective of the exact DGP of the data. They can be competitive models under uncertain situations in the data, where very little is known beforehand or with other practical situations such as short series or heterogeneity across series. This is evident in Tables 10 and 11 where LGBMs and RNNs perform best under many scenarios. However, with RNNs, this superior performance comes at the cost of more computational time as previously seen in Table 20. LGBMs, on the other hand, are catching up with RNNs in terms of their performance, while being extremely fast in model training & testing.

7. Conclusions

The recent work by [Montero-Manso and Hyndman \(2020\)](#) has shown that any local method applied on a dataset of many series can be approximated by a global model with sufficient complexity, irrespective of the relatedness of the underlying series. Therefore, for global models it is about finding the right amount of complexity to outperform local methods. As the complexity of the local models grows with the size of the dataset, whereas for global models it remains constant, global models can afford to be more complex than local models, with less risk of overfitting. However, in practice there are complex trade-offs to be made between model complexity and capabilities on the one hand, and factors such as the availability of data, complexity of DGPs, and the heterogeneity of the underlying data on the other hand. In this work, we have explored in an extensive experimental study some of the poorly understood factors that contribute to global forecasting model performance under these trade-offs. We have focused on characteristics common in real-world forecasting problems and their

related challenges such as series with short history, heterogeneity of the series in one dataset as well as situations where little prior knowledge is available about the underlying patterns of the series, and how we can perform forecasting reasonably well in such circumstances. Through extensive empirical evaluations carried out within a controlled setting of simulated datasets, having desired characteristics, we have demonstrated the interplay between the different aspects that can affect the performance of global forecasting models.

Our methodology involves simulating datasets using a number of DGPs having diverse characteristics. For this, we start by simulating data using the arguably simplest DGPs available and then making them more complex. Thus, we vary the complexity of the DGPs by starting with simple, linear AR(3) and SAR(1) DGPs and then moving onto more complex, non-linear DGPs with the Chaotic Logistic Map, SETAR, and Mackey-Glass Equations. The DGPs that we have used are representative of many real-world phenomena, which are prevalent in use. We simulate both homogeneous and heterogeneous scenarios. In the homogeneous setup, all time series in the dataset are simulated using the same DGP, whereas in the heterogeneous case, time series from different DGPs are mixed together within the same dataset. The availability of data for the experiments is controlled by changing the lengths and the number of series within the datasets. For each scenario, 100 or 1000 datasets are simulated using different random seeds, to achieve reliable and significant experimental results. Similar to the complexity of the DGPs, the complexity of the forecasting techniques is regulated by experimenting using a number of forecasting techniques with different modelling capabilities. We have used linear AR, PR models as well as more complex SETAR, RNNs, FFNNs, and LGBMs as forecasting techniques. The complexity of these models is further varied by introducing two model setups, GFM.All and GFM.GroupFeature, as global model variants. Here, the GFM.All variant learns from all the series, whereas the GFM.GroupFeature variant uses an additional indicator to represent the group within the dataset, in case of induced heterogeneity.

The results of our study have first confirmed that local linear models such as AR work best with known linear patterns in the data, with sufficient lengths in the series. Furthermore, the linear global models such as PR can cope well under multiple short series. Nevertheless, when the patterns are made more complex, the complex non-linear global models such as RNNs, LGBMs are superior to simple linear global models. Furthermore, with heterogeneity existing across series, complex non-linear global models are competitive over linear global models irrespective of the simplicity or complexity of the individual patterns of the series. Thus, non-linear, non-parametric models such as RNNs and LGBMs are in general quite competitive models across a variety of uncertain situations, where we have little prior knowledge about the data. The LGBM models hold another advantage of being computationally efficient models compared to RNNs. Simple models such as AR and PR make assumptions about the linearity of the underlying data. Such assumptions are not always valid and can have a detrimental impact in situations with data having complex patterns. The results of the experiments that involve different scales of heterogeneity prove that the complexity of global forecasting models can be further improved by incorporating prior knowledge about the heterogeneity of data in the form of external features. With respect to data availability, unsurprisingly all global models gradually improve as the lengths and the number of series in the dataset increase. For local models, this improvement is understandably only seen with the length of the individual series. This is because, local models build one model per each time series in the dataset. The model complexity of local models grows proportional to the number of series in the dataset, potentially even higher than the constant complexity of a global model built on the same dataset. This is why, even though fitting a single local model on just one series may take very little time, fitting many of them on a whole dataset of series takes a considerable amount of time.

In terms of future work, further experiments can be conducted across all DGPs by changing the order of the same forecasting models within the same scenarios and evaluating how it affects the performance. As for the heterogeneous setups, a third model setup GFM.Cluster can be introduced which trains multiple GFMs on the different clusters of the same dataset and evaluate whether it improves beyond the GroupFeature setup.

Acknowledgment

This research was supported by the Australian Research Council under grant DE190100045, Facebook Statistics for Improving Insights and Decisions research award, Monash University Graduate Research funding and MASSIVE - High performance computing facility, Australia.

References

- Abadi, M., Agarwal, A., Barham, P., Brevdo, E., Chen, Z., Citro, C., Corrado, G. S., Davis, A., Dean, J., Devin, M., Ghemawat, S., Goodfellow, I., Harp, A., Irving, G., Isard, M., Jia, Y., Jozefowicz, R., Kaiser, L., Kudlur, M., Levenberg, J., Mané, D., Monga, R., Moore, S., Murray, D., Olah, C., Schuster, M., Shlens, J., Steiner, B., Sutskever, I., Talwar, K., Tucker, P., Vanhoucke, V., Vasudevan, V., Viégas, F., Vinyals, O., Warden, P., Wattenberg, M., Wicke, M., Yu, Y., Zheng, X., 2015. TensorFlow: Large-scale machine learning on heterogeneous systems. Software available from tensorflow.org.
URL <https://www.tensorflow.org/>
- Bandara, K., Bergmeir, C., Campbell, S., Scott, D., Lubman, D., 2020a. Towards accurate predictions and causal 'what-if' analyses for planning and policy-making: A case study in emergency medical services demand.
- Bandara, K., Bergmeir, C., Smyl, S., 2020b. Forecasting across time series databases using recurrent neural networks on groups of similar series: A clustering approach. *Expert Systems with Applications* 140, 112896.
- Bandara, K., Shi, P., Bergmeir, C., Hewamalage, H., Tran, Q., Seaman, B., 2019. Sales demand forecast in e-commerce using a long short-term memory neural network methodology. In: Gedeon, T., Wong, K. W., Lee, M. (Eds.), *Neural Information Processing*. Springer International Publishing, Cham, pp. 462–474.
- Ben Taieb, S., Bontempi, G., Atiya, A., Sorjamaa, A., 2012. A review and comparison of strategies for multi-step ahead time series forecasting based on the nn5 forecasting competition. *Expert Systems with Applications* 39 (8), 7067–7083.
- Bergmeir, C., Benítez, J. M., 2012. On the use of cross-validation for time series predictor evaluation. *Information Sciences* 191, 192 – 213, data Mining for Software Trustworthiness.
- Bergmeir, C., Costantini, M., Benítez, J. M., 2014. On the usefulness of cross-validation for directional forecast evaluation. *Computational Statistics & Data Analysis* 76, 132 – 143, cFEnetwork: The Annals of Computational and Financial Econometrics.
- Bergmeir, C., Hyndman, R. J., Koo, B., 2018. A note on the validity of cross-validation for evaluating autoregressive time series prediction. *Computational Statistics & Data Analysis* 120, 70 – 83.
- Bojer, C. S., Meldgaard, J. P., 2020. Kaggle forecasting competitions: An overlooked learning opportunity. *International Journal of Forecasting*.
- Box, G., Jenkins, G., Reinsel, G., 1994. *Time Series Analysis: Forecasting and Control*. Forecasting and Control Series. Prentice Hall.
- Brockwell, P. J., Davis, R. A., 1991. *Time Series: Theory and Methods*. Springer New York.
- Chen, T., Guestrin, C., 2016. Xgboost: A scalable tree boosting system. In: *Proceedings of the 22nd ACM SIGKDD International Conference on Knowledge Discovery and Data Mining. KDD '16*. Association for Computing Machinery, New York, NY, USA, p. 785–794.

- Claveria, O., Torra, S., 2014. Forecasting tourism demand to catalonia: Neural networks vs. time series models. *Economic Modelling* 36, 220 – 228.
- Cryer, J., Chan, K., 2008. *Time Series Analysis: With Applications in R*. Springer Texts in Statistics. Springer.
- eResearch Centre., M., 2019. M3 user guide.
URL <https://docs.massive.org.au/index.html>
- Fabio Di Narzo, A., Luis Aznarte, J., Stigler, M., 2019. tsDyn: Nonlinear Time Series Models with Regime Switching. R package version 0.9-48.1.
URL <https://CRAN.R-project.org/package=tsDyn>
- Fischer, T., Krauss, C., Treichel, A., 2018. Machine learning for time series forecasting - a simulation study. *FAU Discussion Papers in Economics* 02/2018, Friedrich-Alexander University Erlangen-Nuremberg, Institute for Economics.
- García, S., Fernández, A., Luengo, J., Herrera, F., 2010. Advanced nonparametric tests for multiple comparisons in the design of experiments in computational intelligence and data mining: Experimental analysis of power. *Information Sciences* 180 (10), 2044 – 2064, special Issue on Intelligent Distributed Information Systems.
- Gers, F. A., Schraudolph, N. N., Schmidhuber, J., Mar. 2003. Learning precise timing with lstm recurrent networks. *J. Mach. Learn. Res.* 3 (null), 115–143.
- He, K., Zhang, X., Ren, S., Sun, J., June 2016. Deep residual learning for image recognition. In: *2016 IEEE Conference on Computer Vision and Pattern Recognition (CVPR)*. pp. 770–778.
- Hewamalage, H., Bergmeir, C., Bandara, K., 2020. Recurrent neural networks for time series forecasting: Current status and future directions. *International Journal of Forecasting*.
- Hutter, F., Hoos, H. H., Leyton-Brown, K., 17–21 Jan 2011. Sequential model-based optimization for general algorithm configuration. In: *Coello, C. A. C. (Ed.), Learning and Intelligent Optimization*. Springer Berlin Heidelberg, Berlin, Heidelberg, pp. 507–523.
- Hyndman, R., Athanasopoulos, G., Bergmeir, C., Caceres, G., Chhay, L., O’Hara-Wild, M., Petropoulos, F., Razbash, S., Wang, E., Yasmeeen, F., 2020. forecast: Forecasting functions for time series and linear models. R package version 8.11.
URL <http://pkg.robjhyndman.com/forecast>
- Hyndman, R., Khandakar, Y., 2008. Automatic time series forecasting: The forecast package for R. *Journal of Statistical Software, Articles* 27 (3), 1–22.
- Hyndman, R., Koehler, A., Ord, K., D Snyder, R., 01 2008. *Forecasting with exponential smoothing. The state space approach*. Springer Berlin Heidelberg.
- Hyndman, R. J., Athanasopoulos, G., 2018. *Forecasting: Principles and Practice*, 2nd Edition. OTexts.
URL <https://otexts.com/fpp2/>
- Hyndman, R. J., Koehler, A. B., 2006. Another look at measures of forecast accuracy. *International Journal of Forecasting* 22 (4), 679 – 688.
- Hyndman, R. J., Koehler, A. B., Snyder, R. D., Grose, S., 2002. A state space framework for automatic forecasting using exponential smoothing methods. *International Journal of Forecasting* 18 (3), 439 – 454.

- Januschowski, T., Gasthaus, J., Wang, Y., Salinas, D., Flunkert, V., Bohlke-Schneider, M., Callot, L., 2020. Criteria for classifying forecasting methods. *International Journal of Forecasting* 36 (1), 167 – 177, m4 Competition.
- Kang, Y., Li, F., Hyndman, R. J., 2020a. GRATIS: Generating time series with diverse and controllable characteristics. *Statistical Analysis and Data Mining* 13 (4), 354–376.
- Kang, Y., Li, F., Hyndman, R. J., O’Hara-Wild, M., Zhao, B., 2020b. gratis: GeneRAtIng Time Series with diverse and controllable characteristics. R package version 0.2-1.
URL <https://CRAN.R-project.org/package=gratis>
- Ke, G., Meng, Q., Finley, T., Wang, T., Chen, W., Ma, W., Ye, Q., Liu, T.-Y., 2017. Lightgbm: A highly efficient gradient boosting decision tree. In: Guyon, I., Luxburg, U. V., Bengio, S., Wallach, H., Fergus, R., Vishwanathan, S., Garnett, R. (Eds.), *Advances in Neural Information Processing Systems* 30. Curran Associates, Inc., pp. 3146–3154.
- Kingma, D. P., Ba, J., 7–9 May 2015. Adam: A method for stochastic optimization. In: *3rd International Conference for Learning Representations*. Vol. 1412.
- Kunst, R. M., 2008. Cross validation of prediction models for seasonal time series by parametric bootstrapping. *Austrian Journal of Statistics* 37 (3&4), 271–284.
- Lau, K., Wu, Q., 2008. Local prediction of non-linear time series using support vector regression. *Pattern Recognition* 41 (5), 1539 – 1547.
- Lindauer, M., Eggensperger, K., Feurer, M., Falkner, S., Biedenkapp, A., Hutter, F., 2017. Smac v3: Algorithm configuration in python.
URL <https://github.com/automl/SMAC3>
- Mackey, M. C., Glass, L., 1977. Oscillation and chaos in physiological control systems. *Science* 197 (4300), 287–289.
- Makridakis, S., Spiliotis, E., Assimakopoulos, V., 2020a. The m4 competition: 100,000 time series and 61 forecasting methods. *International Journal of Forecasting* 36 (1), 54 – 74, m4 Competition.
- Makridakis, S., Spiliotis, E., Assimakopoulos, V., 10 2020b. The m5 accuracy competition: Results, findings and conclusions.
URL https://www.researchgate.net/publication/344487258_The_M5_Accuracy_competition_Results_findings_and_conclusions
- Mandal, P., Senjyu, T., Urasaki, N., Funabashi, T., 2006. A neural network based several-hour-ahead electric load forecasting using similar days approach. *International Journal of Electrical Power & Energy Systems* 28 (6), 367 – 373.
- Mannattil, M., 2017. nolitsa. <https://github.com/manu-mannattil/nolitsa>.
- May, R. M., Jun. 1976. Simple mathematical models with very complicated dynamics. *Nature* 261 (5560), 459–467.
- Montero-Manso, P., Hyndman, R. J., 2020. Principles and algorithms for forecasting groups of time series: Locality and globality.
URL <https://arxiv.org/abs/2008.00444>
- Orabona, F., 2017. cocob.
URL <https://github.com/bremen79/cocob>

- Orabona, F., Tommasi, T., 04–09 Dec 2017. Training deep networks without learning rates through coin betting. In: Proceedings of the 31st International Conference on Neural Information Processing Systems. NIPS’17. Curran Associates Inc., USA, pp. 2157–2167.
- Petropoulos, F., Makridakis, S., Assimakopoulos, V., Nikolopoulos, K., 2014. ‘horses for courses’ in demand forecasting. *European Journal of Operational Research* 237 (1), 152 – 163.
- R Core Team, 2020. R: A Language and Environment for Statistical Computing. R Foundation for Statistical Computing, Vienna, Austria.
URL <https://www.R-project.org/>
- Rangapuram, S. S., Seeger, M., Gasthaus, J., Stella, L., Wang, Y., Januschowski, T., 2018. Deep state space models for time series forecasting. In: Proceedings of the 32nd International Conference on Neural Information Processing Systems. NIPS’18. Curran Associates Inc., Red Hook, NY, USA, p. 7796–7805.
- Salinas, D., Flunkert, V., Gasthaus, J., Januschowski, T., 2019. Deepar: Probabilistic forecasting with autoregressive recurrent networks. *International Journal of Forecasting*.
- Schäfer, A. M., Zimmermann, H. G., 10–14 Sep 2006. Recurrent neural networks are universal approximators. In: Proceedings of the 16th International Conference on Artificial Neural Networks - Volume Part I. ICANN’06. Springer-Verlag, Berlin, Heidelberg, pp. 632–640.
- Sen, R., Yu, H.-F., Dhillon, I. S., 2019. Think globally, act locally: A deep neural network approach to high-dimensional time series forecasting. In: Wallach, H., Larochelle, H., Beygelzimer, A., d Alché-Buc, F., Fox, E., Garnett, R. (Eds.), *Advances in Neural Information Processing Systems* 32. Curran Associates, Inc., pp. 4837–4846.
- Smith, A. K., 2019. CombMSC: Combined Model Selection Criteria. R package version 1.4.2.1.
URL <https://CRAN.R-project.org/package=CombMSC>
- Smyl, S., 2020. A hybrid method of exponential smoothing and recurrent neural networks for time series forecasting. *International Journal of Forecasting* 36 (1), 75 – 85, m4 Competition.
- Smyl, S., Kuber, K., 19–22 Jun 2016a. Data preprocessing and augmentation for multiple short time series forecasting with recurrent neural networks. In: 36th International Symposium on Forecasting.
- Smyl, S., Kuber, K., 19–22 Jun 2016b. Data preprocessing and augmentation for multiple short time series forecasting with recurrent neural networks. In: 36th International Symposium on Forecasting.
- Suhartono, Amalia, F. F., Saputri, P. D., Rahayu, S. P., Ulama, B. S. S., jun 2018. Simulation study for determining the best architecture of multilayer perceptron for forecasting nonlinear seasonal time series. *Journal of Physics: Conference Series* 1028, 012214.
- Sun, J., Yang, Y., Liu, Y., Chen, C., Rao, W., Bai, Y., 2019. Univariate time series classification using information geometry. *Pattern Recognition* 95, 24 – 35.
- Svetunkov, I., 2019. smooth: Forecasting Using State Space Models. R package version 2.5.3.
URL <https://CRAN.R-project.org/package=smooth>
- Tong, H., 1978. On a threshold model. In: *Pattern Recognition and Signal Processing*. Springer Netherlands, pp. 575–586.
- Tong, H., Lim, K. S., 1980. Threshold autoregression, limit cycles and cyclical data. *Journal of the Royal Statistical Society: Series B (Methodological)* 42 (3), 245–268.
- Trapero, J. R., Kourentzes, N., Fildes, R., Feb 2015. On the identification of sales forecasting models in the presence of promotions. *Journal of the Operational Research Society* 66 (2), 299–307.

- Vanli, N. D., Sayin, M. O., Mohaghegh N., M., Ozkan, H., Kozat, S. S., 2019. Nonlinear regression via incremental decision trees. *Pattern Recognition* 86, 1 – 13.
- Wang, Y., Smola, A., Maddix, D., Gasthaus, J., Foster, D., Januschowski, T., 09–15 Jun 2019. Deep factors for forecasting. Vol. 97 of *Proceedings of Machine Learning Research*. PMLR, Long Beach, California, USA, pp. 6607–6617.
- Wen, R., Torkkola, K., Narayanaswamy, B., Madeka, D., 2017a. A multi-horizon quantile recurrent forecaster.
URL <https://arxiv.org/abs/1711.11053>
- Wen, R., Torkkola, K., Narayanaswamy, B., Madeka, D., Nov. 2017b. A Multi-Horizon quantile recurrent forecaster. In: *Neural Information Processing Systems*.
- Ye, R., Dai, Q., 2021. Implementing transfer learning across different datasets for time series forecasting. *Pattern Recognition* 109, 107617.
- Zhang, G., Patuwo, B., Hu, M. Y., 2001. A simulation study of artificial neural networks for nonlinear time-series forecasting. *Computers & Operations Research* 28 (4), 381 – 396.
- Zhang, G. P., Dec. 2007. A neural network ensemble method with jittered training data for time series forecasting. *Inf. Sci.* 177 (23), 5329–5346.
- Zhang, G. P., Qi, M., Jan. 2005. Neural network forecasting for seasonal and trend time series. *Eur. J. Oper. Res.* 160 (2), 501–514.
- Zhang, H., Nieto, F. H., 2017. TAR: Bayesian Modeling of Autoregressive Threshold Time Series Models. R package version 1.0.
URL <https://CRAN.R-project.org/package=TAR>
- Zhao, J., Itti, L., 2018. shapedtw: Shape dynamic time warping. *Pattern Recognition* 74, 171 – 184.
- Zhu, L., Laptev, N., Nov 2017. Deep and confident prediction for time series at uber. 2017 IEEE International Conference on Data Mining Workshops (ICDMW).

Appendix A. Results of Data Availability Experiments

Appendix A.1. AR(3) DGP

Length of Series	RNN(3)	FFNN(3)	LGBM(3)	AR(2)	AR(3)	AR(10)
18	23.02	24.82	23.67	18.48	19.26	32.72
36	21.58	21.07	21.77	18.1	18.27	20.62
54	20.54	21.12	21.59	18.08	18.3	19.77
72	19.16	21.57	21.72	17.94	18.02	18.93
90	19.62	20.36	20.61	17.71	17.85	18.9
180	19.41	19.46	19.99	17.63	17.66	18
360	18.84	18.7	19.1	16.67	16.69	16.9
540	19.99	20.09	19.35	17.5	17.48	17.58
720	17.89	19.22	19.61	17.45	17.47	17.62
900	19.06	18.86	19.29	17.17	17.2	17.25
1,350	18.53	19.44	19.87	17.87	17.86	17.92
1,800	18.04	19.11	19.25	17.48	17.47	17.55

Table A.1: Mean SMAPE Results for AR(3) DGP SS Scenario

No. of Series	RNN(3)	FFNN(3)	LGBM(3)	AR(2)	AR(3)	AR(10)	PR(10)	PR(3)
1	23.06	23.32	23.67	18.48	19.25	32.72	83.30	20.65
2	20.44	22.04	21.95	19.01	19.49	31.51	96.31	18.69
3	20.45	21.02	20.98	19.27	20.04	33.29	35.80	18.87
4	19.88	20.60	21.26	18.95	19.59	31.72	26.36	18.35
5	19.72	20.36	20.73	19.07	19.77	33.30	23.11	18.27
10	19.00	19.68	20.25	18.90	19.33	33.07	19.99	17.94
20	18.10	18.78	19.51	18.26	19.20	32.95	18.41	17.08
30	18.40	19.19	19.53	18.85	19.40	32.19	18.45	17.83
40	18.19	19.25	19.65	19.14	19.76	32.31	18.63	17.86
50	18.08	18.94	19.23	18.45	19.12	33.72	18.15	17.55
75	18.58	19.53	19.86	19.57	20.04	32.32	18.61	18.13
100	18.12	18.91	19.25	18.79	19.53	32.92	18.15	17.71

Table A.2: Mean SMAPE Results for AR(3) DGP MS-Hom-Short Scenario

Length of Series	RNN(10)	RNN(3)	FFNN(10)	FFNN(3)	LGBM(10)	LGBM(3)	AR(2)	AR(3)	AR(10)	PR(10)	PR(3)
18	-	-	-	-	-	-	22.71	23.44	39.29	22.02	21.43
36	21.46	21.70	21.87	22.98	22.03	23.36	21.73	22.05	24.98	21.28	21.20
54	21.32	21.43	21.82	22.96	21.89	23.26	21.44	21.63	23.38	21.15	21.11
72	21.26	21.45	21.84	22.98	21.84	23.19	21.36	21.49	22.68	21.13	21.11
90	21.25	21.35	21.77	22.91	21.74	23.08	21.22	21.33	22.25	21.04	21.03
108	21.22	21.59	21.69	23.03	21.75	23.10	21.22	21.31	22.06	21.07	21.06
126	21.22	21.36	21.84	23.00	21.74	23.07	21.22	21.30	21.92	21.10	21.09
144	21.32	21.40	21.81	22.96	21.69	23.03	21.15	21.22	21.77	21.04	21.04
162	21.14	21.26	21.62	22.95	21.67	23.01	21.14	21.19	21.64	21.03	21.03
180	21.22	21.37	21.84	23.06	21.72	23.07	21.17	21.22	21.63	21.08	21.07

Table A.3: Mean SMAPE Results for AR(3) DGP MS-Hom-Long Scenario

Length of Series	RNN(10)	RNN(3)	FFNN(10)	FFNN(3)	LGBM(10)	LGBM(3)	AR(2)	AR(3)	AR(10)	PR(10)	PR(3)
18	-	-	-	-	-	-	21.72	22.51	36.98	24.40	22.59
36	22.02	22.19	22.70	23.49	22.39	23.59	20.60	20.89	23.77	22.19	21.98
54	21.94	22.10	22.21	23.37	22.19	23.49	20.28	20.44	22.12	21.96	21.88
72	21.01	21.83	21.99	23.52	22.02	23.34	20.14	20.25	21.39	21.78	21.75
90	20.89	21.90	22.39	23.30	21.90	23.28	20.00	20.08	20.93	21.70	21.68
108	20.84	21.83	22.04	23.27	21.92	23.31	20.00	20.06	20.76	21.74	21.73
126	21.11	21.83	21.88	23.42	21.89	23.26	19.95	19.98	20.58	21.71	21.70
144	21.02	21.00	22.08	23.28	21.81	23.25	19.91	19.93	20.44	21.65	21.64
162	20.71	21.89	21.94	23.39	21.77	23.18	19.90	19.92	20.37	21.64	21.64
180	20.88	21.78	22.21	23.35	21.85	23.29	19.93	19.95	20.34	21.72	21.72

Table A.4: Mean SMAPE Results for AR(3) DGP MS-Het Scenario

Appendix A.2. SAR(1) DGP

Length of Series	RNN(12)	FFNN(12)	LGBM(12)	AR(12)	AR(3)	SAR(1)
24	9.14	10.35	11.31	7.92	9.29	5.09
48	6.17	6.37	9.71	5.68	8.90	5.12
72	6.17	7.55	8.86	5.34	8.82	4.93
96	5.48	5.43	6.88	5.21	8.86	4.98
120	5.40	5.35	6.17	5.10	8.77	4.92
240	5.19	7.42	5.60	5.04	9.06	4.89
480	5.80	6.93	5.34	4.98	9.17	4.94
720	5.19	5.95	5.37	4.94	9.42	4.91
960	7.41	6.82	5.10	4.80	9.02	4.76
1,200	7.47	5.16	5.19	4.96	9.01	4.93
1,800	5.02	6.79	5.19	4.92	9.00	4.91
2,400	4.91	4.94	5.00	4.77	8.86	4.75

Table A.5: Mean SMAPE Results for SAR(1) DGP SS Scenario

No. of Series	RNN(12)	FFNN(12)	LGBM(12)	AR(12)	AR(3)	SAR(1)	PR(12)
1	9.46	10.40	11.31	7.92	9.29	5.09	73.11
2	10.14	10.54	10.40	8.01	9.30	5.20	12.37
3	8.14	8.97	8.68	8.18	9.12	5.06	8.02
4	9.09	7.82	8.17	7.97	9.13	5.06	6.86
5	7.04	7.10	7.63	7.88	9.08	5.04	6.31
10	6.01	5.85	6.65	7.61	9.21	5.00	5.62
20	5.50	5.35	6.11	7.82	9.11	5.07	5.38
30	5.53	5.26	6.00	8.00	9.22	5.03	5.27
40	5.07	5.18	5.48	8.08	9.05	4.90	5.06
50	5.09	5.05	5.50	7.79	9.04	5.00	5.19
75	5.08	5.06	5.39	7.99	9.07	5.10	5.10
100	4.90	4.86	5.19	7.69	8.88	4.90	4.93

Table A.6: Mean SMAPE Results for SAR(1) DGP MS-Hom-Short Scenario

Length of Series	RNN(12)	FFNN(12)	LGBM(12)	AR(12)	AR(3)	SAR(1)	PR(12)
24	14.33	14.34	15.16	22.76	25.13	14.41	14.51
96	13.52	13.47	13.63	14.24	23.44	13.43	13.51
144	13.26	13.29	13.36	13.76	23.32	13.23	13.27
192	13.22	13.20	13.30	13.55	23.33	13.18	13.20
240	14.03	13.22	13.29	13.49	23.40	13.18	13.19

Table A.7: Mean SMAPE Results for SAR(1) DGP MS-Hom-Long Scenario

Length of Series	RNN(12)	FFNN(12)	LGBM(12)	AR(12)	AR(3)	SAR(1)	PR(12)
24	23.01	23.20	23.08	33.14	23.70	22.88	23.16
96	22.26	22.99	22.91	22.59	22.31	21.35	22.10
144	22.21	22.96	22.85	22.00	22.16	21.23	22.02
192	22.21	23.05	22.88	21.77	22.14	21.22	22.03
240	22.15	22.98	22.84	21.65	22.11	21.20	22.02

Table A.8: Mean SMAPE Results for SAR(1) DGP MS-Het Scenario

Appendix A.3. Chaotic Logistic Map DGP

Length of Series	RNN(15)	FFNN(15)	LGBM(15)	AR(15)
60	64.44	63.86	58.97	57.27
180	56.38	54.17	52.33	52.54
300	54.64	55.10	53.75	53.98
1,200	49.99	50.25	49.32	52.00
2,400	51.17	51.45	50.31	53.65
4,500	51.78	52.59	48.85	52.75
6,000	51.63	53.27	48.93	52.91

Table A.9: Mean SMAPE Results for Chaotic Logistic Map DGP SS Scenario

No. of Series	RNN(15)	FFNN(15)	LGBM(15)	AR(15)	PR(15)
1	62.87	65.36	58.80	57.27	63.69
3	55.26	53.90	53.40	56.52	53.72
5	56.66	56.56	55.18	57.49	54.72
20	51.78	51.64	50.58	56.51	52.32
40	53.42	52.04	51.32	57.53	54.10
75	49.76	51.31	49.99	56.54	53.03
100	49.21	50.15	50.43	57.67	53.37

Table A.10: Mean SMAPE Results for Chaotic Logistic Map DGP MS-Hom-Short Scenario

Length of Series	RNN(15)	FFNN(15)	LGBM(15)	AR(15)	PR(15)
60	49.45	50.47	49.30	56.73	52.94
240	48.10	50.65	47.26	52.98	52.52
360	48.22	50.43	47.09	52.81	52.53
480	48.07	50.08	46.99	52.80	52.58
600	48.12	47.50	46.80	52.65	52.46

Table A.11: Mean SMAPE Results for Chaotic Logistic Map DGP MS-Hom-Long Scenario

Length of Series	RNN(15)	FFNN(15)	LGBM(15)	AR(15)	PR(15)
60	28.34	28.79	28.36	30.61	28.26
240	27.47	28.31	27.68	27.94	27.75
360	27.37	28.84	27.58	27.74	27.70
480	28.02	28.60	27.52	27.61	27.63
600	27.54	28.18	27.45	27.56	27.63

Table A.12: Mean SMAPE Results for Chaotic Logistic Map DGP MS-Het Scenario